Available online at www.sciencedirect.com
SCIENCE DIRECT
Tectonophysics 412 (2006) 1–25
TECTONOPHYSICS
www.elsevier.com/locate/tecto

Cenozoic cooling histories in the Menderes Massif, western Turkey, may be caused by erosion and flat subduction, not low-angle normal faulting

Rob Westaway

Faculty of Mathematics and Computing, The Open University, Eldon House, Gosforth, Newcastle-upon-Tyne NE3 3PW, UK

Received 29 June 2004; received in revised form 5 December 2004; accepted 7 August 2005
Available online 20 October 2005

Abstract

Since the early 1990s, a prolific literature has developed on the interpretation within western Turkey of apparent Mid to Late Cenozoic low-angle normal faults. Extension on these structures has been thought responsible for the exhumation of this region's principal metamorphic massif, the Menderes Massif, which has thus been interpreted as a metamorphic core complex. Nonetheless, no convincing supporting structural evidence has emerged: some reported instances of low-angle normal faulting affecting the Menderes Massif can be shown from field relationships to have formed as steep normal faults and to have since become back-tilted; others seem to be misinterpretations of structures with no demonstrable relationship to extension at all. The main evidence for low-angle normal faulting in this region has instead emerged through thermochronology, which indicates highly non-uniform cooling histories that have seemed to lack any other explanation. However, this evidence can alternatively be explained by a combination of the cooling effects caused by flat subduction and by erosion. There is thus no evidence for Cenozoic low-angle normal faulting affecting the Menderes Massif. Extension started at ~11 Ma in parts of western Turkey; but most of this region's Late Cenozoic extension—on normal faults with steep initial dips—has occurred since ~7 Ma, synchronous with slip on the North Anatolian Fault Zone.

Keywords: Turkey; Extension; Low-angle normal faulting; Cenozoic; Denudation; Thermochronology; Subduction

1. Introduction

In the eastern part of the Aegean extensional province in western Turkey, active normal fault zones (notably the north-dipping Alaşehir Fault Zone or AFZ and the south-dipping Büyük Menderes Fault Zone or BMFZ; Fig. 1) cut through metamorphic rocks of the Menderes Massif. Over the past decade, possible relationships between the metamorphic fabrics evident in this massif and this region's present phase of crustal extension have been intensively researched. This active extension occurs on steep normal faults, with typical dips of ~40–60° (e.g., Jackson, 1987; Jackson and White, 1989; Westaway, 1990, 1994b, 1998). However, a popular view has arisen, that this extension has developed from an earlier phase of low-angle normal faulting, involving many tens of kilometres of slip on normal faults that formed at dips of ~30° or less, which exhumed the Menderes Massif (e.g., Hetzel et al., 1995a,b), thus leading to the suggestion that this is "the world's largest metamorphic core complex" (cf. Verge, 1993).

Diverse forms of evidence have been proposed in support of this low-angle normal faulting, including interpretations of fabrics in the metamorphic basement,

E-mail address: robwestaway@tiscali.co.uk.

0040-1951/$ - see front matter © 2005 Elsevier B.V. All rights reserved.
doi:10.1016/j.tecto.2005.08.005

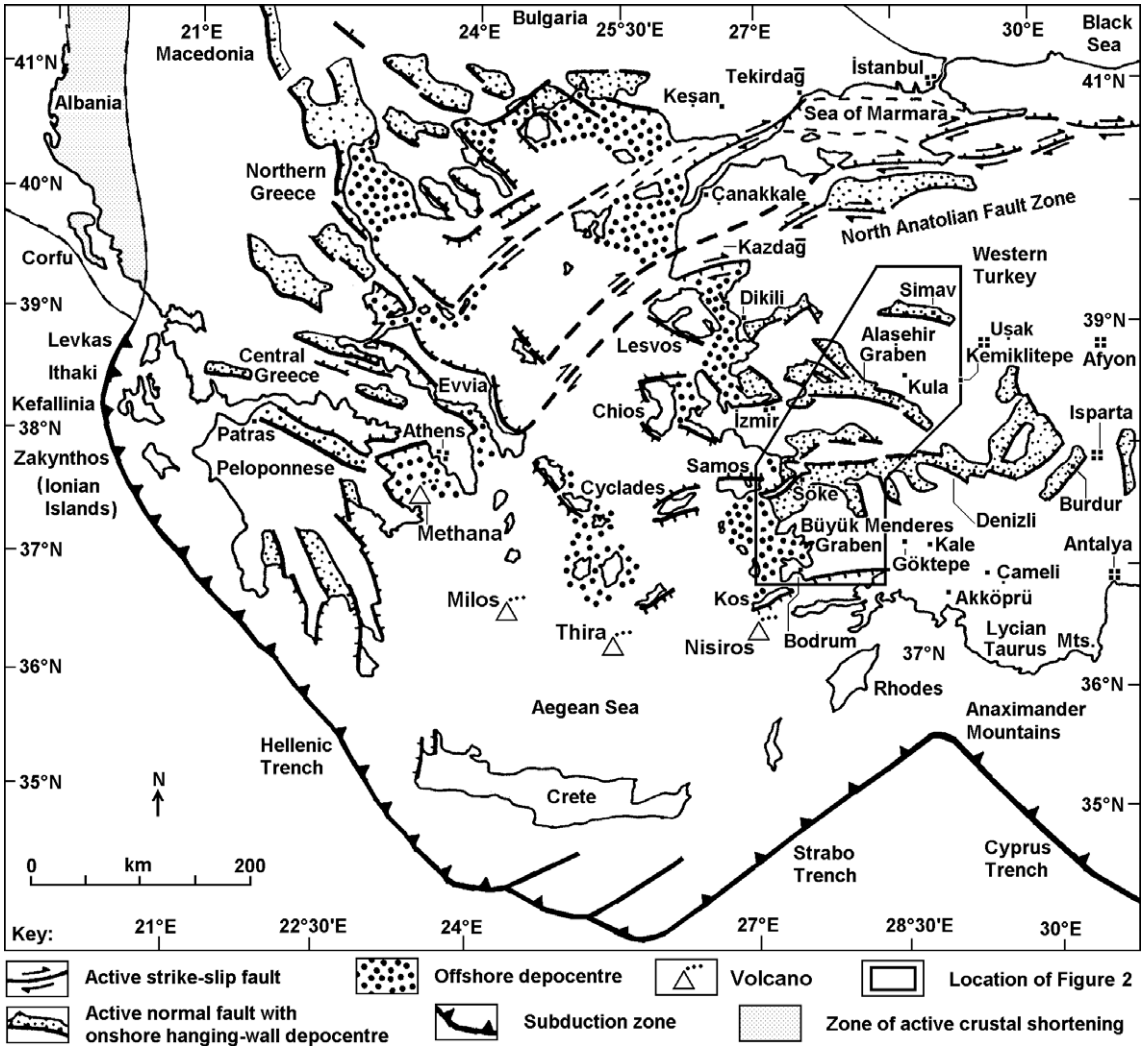

Fig. 1. Map of western Turkey showing the location of Fig. 2 in relation to active normal fault zones and sites of Late Miocene alkali-basaltic volcanism that is considered extension-related (e.g., Aldanmaz et al., 2000). A compilation of K–Ar and Ar–Ar dates by Westaway et al. (2005) indicates that the earliest evidence of extension is provided by volcanism in the extreme west of Turkey at ~11 Ma, around Çanakkale (the Taştepe volcanics) and west of İzmir (the Urla volcanics). Volcanism subsequently rapidly spread north, east and south until it covered most of the modern extensional province by ~7 Ma. The brief phase of volcanism in the Denizli area at ~7 Ma is thought to mark the start of local extension (Westaway et al., 2005) and matches the thermochronologic estimate of the start of extension in the Alaşehir Graben obtained in this study. The North Anatolian Fault Zone is also now thought to have become active at ~7 Ma (e.g., Westaway, 2003, 2004a); accommodating its right-lateral slip has required rollback of the Hellenic subduction zone and extension of the overlying plate (cf. Meijer and Wortel, 1997).

isotopic dating, and thermochronologic evidence (see below). However, the significance of much of this evidence has been disputed. For instance, at one stage it was argued that there is a characteristic progressive upward gradation in footwall regions between ductile and brittle fabrics in this basement (cf., Bozkurt and Park, 1994), implying that "tectonic denudation" by low-angle normal faulting caused progressive exhumation of the present footwall regions from mid-crustal depths. Such a transition is observed in the footwall of the AFZ (e.g., Hetzel et al., 1995b), but this is a steep normal fault zone that has been back-tilted, not a low-angle one (see below). Elsewhere, this interpretation was later challenged (e.g., Hetzel and Reischmann, 1996), and the resulting reinterpretation involved no direct connection between older ductile fabrics and much younger brittle faulting. The issue of whether abrupt changes in metamorphic grade occur, between "footwalls" and "hanging-walls" of interpreted ductile extensional shear zones, continues to be disputed (cf. Bozkurt, 2001a,b, 2004; Erdoğan and Güngör, 2004) and is thus not clearly demonstrated, either. The pres-

ence of subhorizontal foliations in the metamorphic basement has been used in many studies to infer low-angle normal faulting, it being stated that they are always precisely parallel to the land surface or inferred detachment surface, which is thus interpreted as a low-angle normal fault plane. However, there has been no convincing demonstration that such fabrics die out downwards as would be expected if they formed by ductile deformation at mid-crustal depths in the footwall of a low-angle normal fault. In some cases it has also been realised (e.g., by Purvis and Robertson, 2004) that these fabrics are in fact oblique to the land surface that has been interpreted as the footwall of a low-angle normal fault, undermining the original argument.

It has also been persistently argued that granite intrusion in western Turkey has been synkinematic with low-angle normal faulting (e.g., Hetzel et al., 1995a,b; Bozkurt, 2004). However, this region's history of granite intrusion and subsequent metamorphism has been complex, with indications of Late Precambrian granites related to crustal consolidation (e.g., Hetzel and Reischmann, 1996; Gessner et al., 2001a), Triassic granites related to a continental collision (e.g., Koralay et al., 2001), and Oligocene granites that post-date the final closure of the Neotethyan ocean basins and may thus be related to thickening of the continental crust (e.g., Erdoğan and Güngör, 2004) or incipient subduction of the Hellenic slab. The latter granites have also been interpreted as syn-extensional (e.g., Bozkurt, 2004) but this interpretation is not universally accepted (cf. Erdoğan and Güngör, 2004). A single late Early Miocene Ar–Ar date of 19.5 ± 1.4 Ma for amphibole in granite in the AFZ footwall stimulated the development of hypotheses with granite intrusion synkinematic with low-angle normal faulting, with both processes occurring in the Middle Miocene (cf., Hetzel et al., 1995a,b). Although it was promptly argued that this date may mark cooling through closure conditions for argon retention, rather than being an intrusion age (Westaway, 1996), this idea was dismissed as ridiculous (Hetzel et al., 1996). However, there is no structural evidence that this granite intruded during extension on this normal fault system; the fact that it carries a pervasive ductile deformation fabric that is shared by the surrounding metamorphic rocks and relates to young extension, but no earlier fabric (cf. Hetzel et al., 1995b), does not mean that it intruded synkinematically, just that it intruded after the earlier fabrics had developed. The dating is likewise contentious, as its argon release spectrum and isochron plot were both obtained by discarding data from the majority of sample splits from different heating steps (see Hetzel et al., 1995b, Figs. 12 and 13), most of this discarded data and some of the data that were included being consistent with much greater ages. The justification for discarding this data was possible inheritance of argon or young alteration (cf. Hetzel et al., 1995b), but these explanations are contradictory, and it makes no sense to suggest that amphibole that crystallised during granite intrusion could contain inherited argon, as the crystallisation temperature is much higher than the closure temperature for argon retention. In contrast, argon retention in metamorphosed or thermally disturbed amphiboles can be extremely difficult to interpret, with argon uptake being sometimes observed (cf. McDougall and Harrison, 1999, pp. 28–29). The complex argon spectra observed in this one sample thus raise the possibility that it has been metamorphosed, from which it follows that the intrusion of this granite had no demonstrable connection with any Miocene normal faulting and the Miocene date is thus a cooling age, as previously suggested (Westaway, 1996). Similar arguments affect the inference of Late Oligocene/Early Miocene low-angle normal faulting in relation to granite intrusion in the Simav area farther north (cf. Işik and Tekeli, 2001).

Another argument against the existence of low-angle normal faulting is provided by geometrical relationships between dips of normal faults and those of the oldest sediments deposited adjacent to them, which either mark or pre-date the start of extension (see, also, e.g., Gessner et al., 2001b; Bozkurt, 2000, 2003). For instance, using the data from Purvis and Robertson (2004), the so-called "detachment" bounding the AFZ has a typical present-day dip of ~16°, and the oldest sediments in its hanging-wall (which may pre-date the start of extension on it; e.g., Bozkurt, 2000) dip at up to ~60°. The initial dip of this normal fault can thus be estimated using the standard vertical shear technique of Westaway and Kusznir (1993), and is ~64°. It thus now seems clear that what have been regarded for a time as the most obvious low-angle normal faults, those apparently related to the AFZ, dipping north, and to the BMFZ, dipping south (cf., Hetzel et al., 1995a,b), first developed as steep normal faults, and became back-tilted in part as a result of their own slip and in part through slip on other sets of normal faults that developed later (cf. Westaway, 1998). This is, of course, how such structures were interpreted in the first place (cf. Proffett, 1977; Jackson and McKenzie, 1983), before the possibility of low-angle normal faulting was suggested. Gessner et al. (2001b) and Ring et al. (2003) estimated using similar geometric calculations to those above that their "Güney Detachment" associated with the BMFZ formed with an initial dip of ~40° and that their "Kuzey Detachment" associated

with the AFZ formed with an initial dip of ~60°. They thus accepted that the active normal faulting in the AFZ, at least, developed with a steep initial dip, in which case it makes no sense to refer to this structure as containing a "detachment", since this term implies a low-angle initial dip. However, Ring et al. (2003) estimated that their "Simav Detachment", north of the AFZ (Fig. 2), formed with a probable initial northward dip of ~10–20° and that their "Lycian Detachment", south of the BMFZ (Fig. 2), probably had a similar initial south-

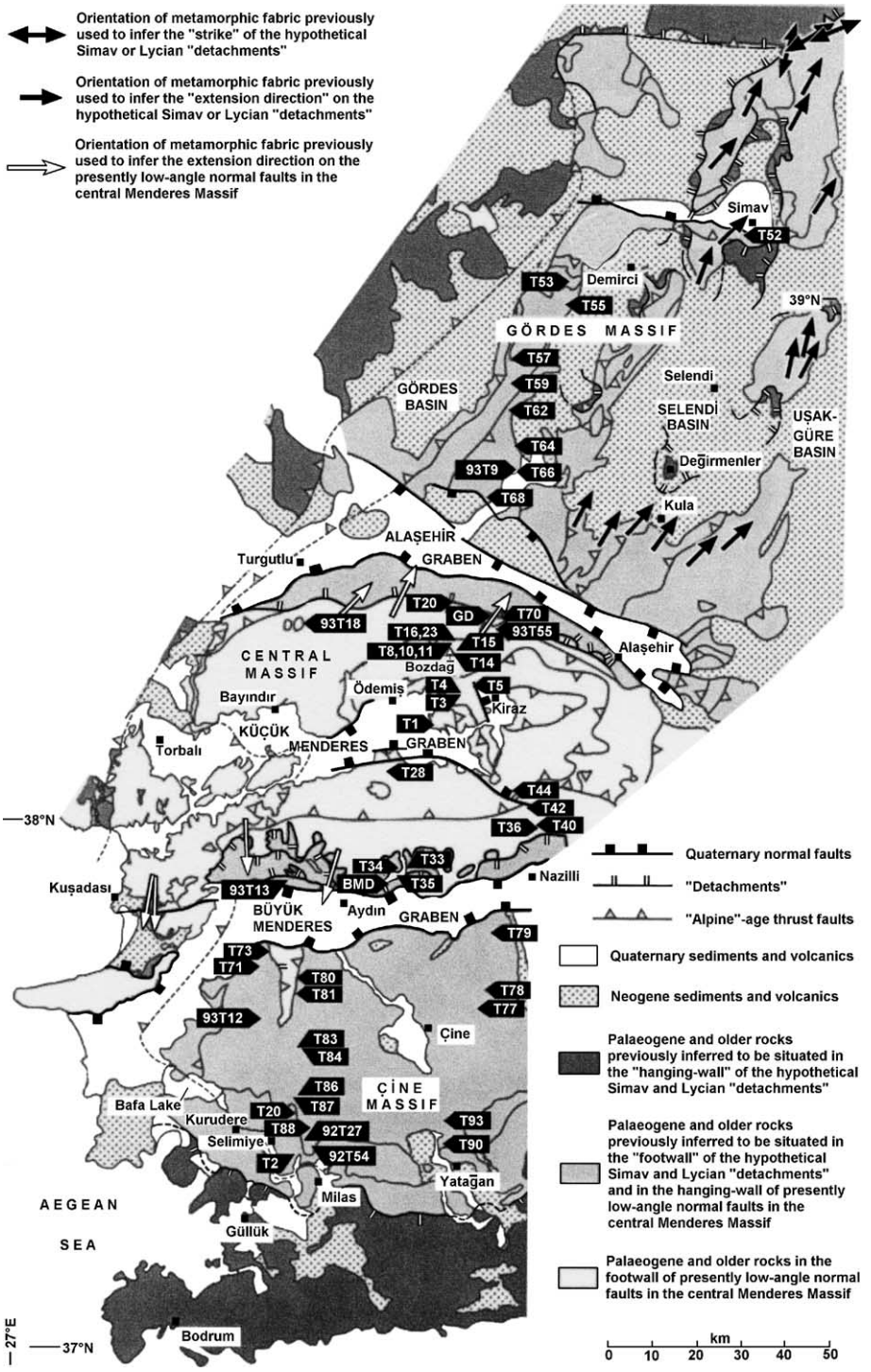

ward dip, making it clear that they regarded these structures as true low-angle normal fault zones.

An additional argument against the possibility of mid-Cenozoic low-angle normal faulting in western Turkey arises from consideration of the form of the stress field required to permit this process. In general, it is mechanically very difficult to form any low-angle normal fault, because it will be strongly misaligned relative to any conventional extensional stress field with a vertical maximum principal stress. For the stress field to be inclined at depth requires atypical conditions, which only seem possible in continental crust that is cold (<~300–350 °C) when extension begins (Westaway, 1999). However, studies of metamorphism (e.g., Rimmelé et al., 2003) and thermochronology (e.g., Ring et al., 2003) indicate that the lower crust of western Turkey was hot (>~500 °C) in the mid-Cenozoic. Despite the proliferation of low-angle normal fault and metamorphic core complex interpretations in the recent literature, the weakness of the underlying evidence has led some authors (e.g., Okay, 2001; Erdoğan and Güngör, 2004) to suggest that the history of the Menderes Massif, between its earlier phase of Oligocene crustal shortening and the young phase of extension that continues to the present day, relates purely to erosion, a view supported by the present study.

The remaining evidence that can support a significant phase of low-angle normal faulting comes from thermochronology (e.g., Ring et al., 2003; Fig. 2); this indicates rapid cooling in the Late Oligocene/Early Miocene (Fig. 3). Although cooling can of course be caused simply by erosion (cf. Westaway, 2002a), the observed very non-uniform cooling rates (Fig. 3) seem to cast doubt on this interpretation. However, elsewhere, notably in both western North America (e.g., Dumitru et al., 1991) and western South America (e.g., Gutscher et al., 2000), it has been deduced that flat subduction will cool the overlying crust and lithosphere, by effectively introducing a second layer of lithosphere. Westaway et al. (2005) tentatively suggested that this process, combined with erosion, may account for the cooling histories observed in western Turkey, thus removing any need for a hypothetical phase of Late Oligocene/Early Miocene or younger low-angle normal faulting. The aims of this study are to present a formal analysis of this problem, which shows that this supposition is tenable, and to examine in detail some example cooling histories from key parts of western Turkey.

2. Preliminary investigations of thermal regimes for western Turkey

One requirement of any model for the thermal history of the continental lithosphere of western Turkey is its ability to account for the present-day conditions. It is well-known that, at present, the surface heat flow in western Turkey is high, typically ~110 mW m^{-2} (e.g., Ilkışık, 1995) and reaching ~120 mW m^{-2} in some localities, such as the Kula Quaternary volcanic field (e.g., Westaway et al., 2004; Fig. 2), requiring a geothermal gradient in the uppermost crust of ~40 °C km^{-1}. Ilkışık (1995) estimated that about half this heat flux (i.e., ~55 mW m^{-2}) arises through radiogenic heat production in the upper crust, the rest being the result of conduction from the Earth's interior. In many regions, the surface heat flow varies linearly with the

Fig. 2. Map of thermochronologic sampling sites in western Turkey, adapted from Fig. 3 of Ring et al. (2003). See other maps, such as Fig. 2c of Ring et al. (2001) for details of which metamorphic units are present in each locality. Diagram is labelled to emphasise the interpretation of 'detachments' favoured by Ring et al. (2003), even though much of this interpretation scheme is now thought to be wrong. This scheme infers north-dipping low-angle normal fault zones in the Kula-Selendi-Simav-Demirci area (their "Gördes detachment") and south of the Alaşehir Graben (their "Kuzey detachment"), and south-dipping low-angle normal fault zones north of the Büyük Menderes Graben (their "Güney detachment") and in the Yatağan-Milas-Güllük area (their "Lycian detachment"). Dark-shaded area in the south indicates the Lycian Nappes structural unit, which is thought to represent material thrust onto surrounding areas of continental crust during the Early to Middle Eocene closure of the Inner Tauride ocean (cf. Garfunkel, 2004), although other interpretations have been proposed (e.g., Collins and Robertson, 1998). Dark-shaded area in the north indicates similar sequences related to Early to Middle Eocene closure of the İzmir-Ankara-Erzincan ocean. Many of these outcrops are readily accessible in the field, such as the Değirmenler inlier near Kula (cf. Seyitoğlu, 1997; Westaway et al., 2004), and provide no evidence for any conceivable interpretation in terms of low-angle normal faulting. In contrast, the "Kuzey detachment" and "Güney detachment" are real normal fault zones that, from field relationships to adjacent sediments, formed with steep dips but have since become back-tilted. The switch to the presently active steeper normal faults in their hanging-walls is constrained from mammalian biostratigraphic evidence to the Early Pleistocene (e.g., Ünay et al., 1995; Ünay and de Bruijn, 1998; Bozkurt, 2000; Sarıca, 2000), consistent with physical modelling of the stress field (Westaway, 1998). The extension directions shown as white arrows apply to the initial set of faults, which are now inactive, but data for the presently active set (e.g., Westaway, 1990, 1994b) are subparallel. Structural studies (e.g., Westaway, 1994b) also indicate many more active normal faults than are shown here, particularly in the western part of the central Menderes Massif. In the Çine Massif, the main structural unit depicted (around Çine itself) represents gneiss, indicating crust that formed and experienced its peak metamorphic conditions during the Late Precambrian Pan-African orogeny; the narrower structural units farther south, around Selimiye, Milas and Yatağan, represent schists that have since been juxtaposed onto the gneiss and yield conditions indicative of the start of cooling in the Early Cenozoic (cf. Gessner et al., 2001c, 2004; Whitney and Bozkurt, 2002). See text for discussion.

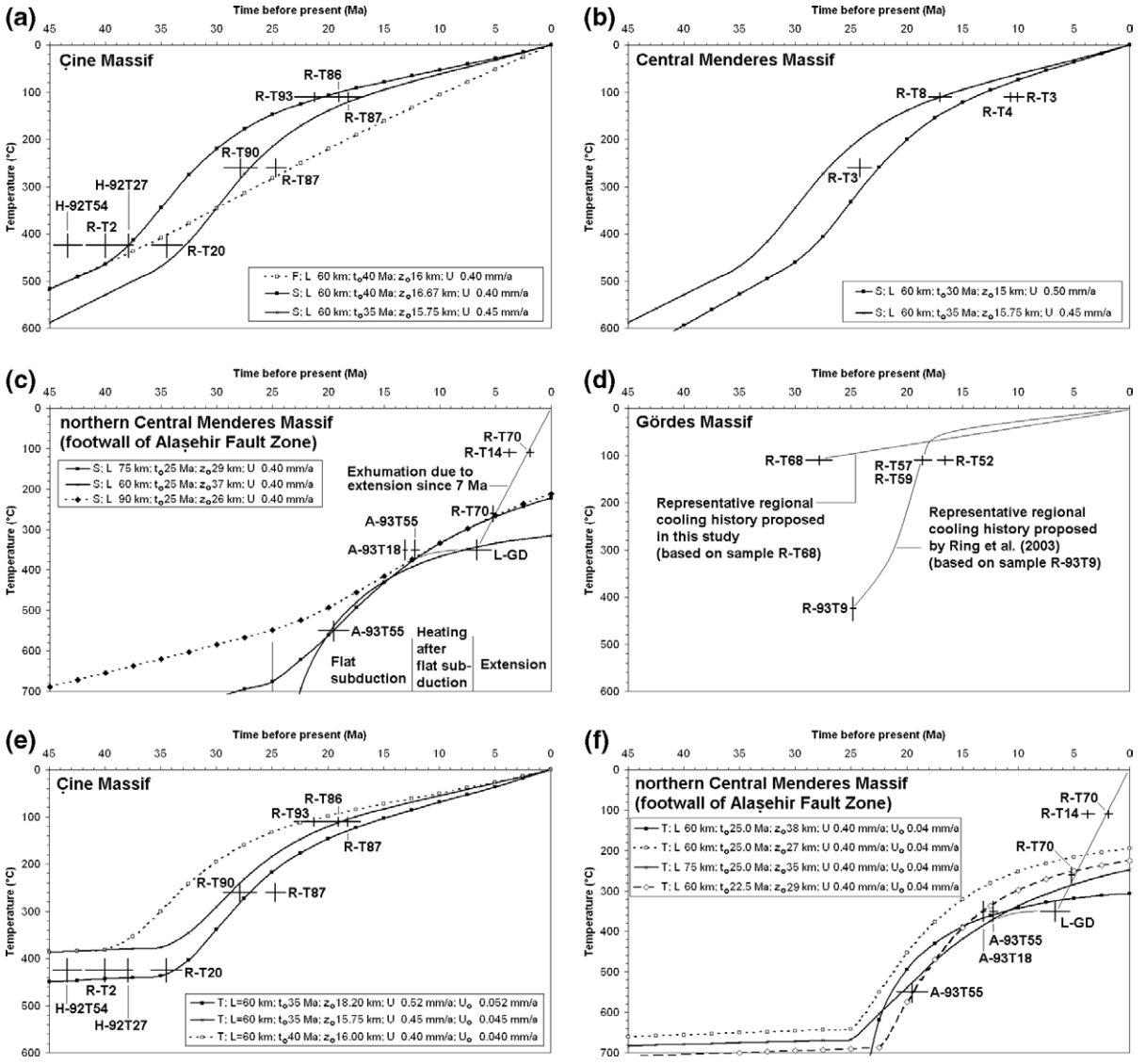

Fig. 3. Comparisons between data and predicted cooling histories (a) for the Çine Massif (b) for the central part of the Central Massif (c) for the northern part of the Central Massif, in the footwall of the Alaşehir fault zone (d) for the Gördes Massif. (e) Revision of (a) to include an increase in erosion rates at the start of flat subduction. (f) Similar revision to (c). Data are from: A, Hetzel et al. (1995b); H, Hetzel and Reischmann (1996); L, Lips et al. (2001); and R, Ring et al. (2003); see Fig. 2 for site locations. Fine lines are sketches of possible cooling histories; other thicker solid and dashed lines are based on calculations using the method developed in this study, using the parameter values indicated in the legend. Predictions labelled F use the solution in Eq. (24), whereas those labelled S use Eq. (29), and those labelled T use Eq. (33). L is the lithosphere thickness; t_o is the start time of subduction; z_o is the depth of the observation point at time t_o; U is the erosion rate for time after t_o; and U_o is the erosion rate before time t_o, where different. See text for discussion.

radiogenic heat production $Z(z=0)=Z_o$ in surface rocks (e.g., Lachenbruch, 1970). The most satisfactory explanation of this relation requires $Z(z)$ to decrease exponentially with depth, as

$$Z(z) = Z_o \exp(-z/D). \quad (1)$$

D quantifies the depth scale of this decrease and is typically ~10 km (e.g., Lachenbruch, 1970). A linear increase in heat flow with Z_o could instead involve $Z(z)=Z_o$ throughout the crust. However, in many regions Z_o is so high that if $Z(z)=Z_o$ all the surface heat flow would be produced in the crust such that the conductive component q_o through the mantle lithosphere would have to be zero. A possible explanation for the exponential decay in $Z(z)$, suggested by Lachenbruch (1970) and others, is that hydrothermal circulation concentrates radioactive elements towards the upper part of the crust.

If radiogenic heat production varies as in Eq. (1), then the temperature (in the absence of denudation or sedimentation) satisfies

$$T_z = \frac{q_o z}{k} + \frac{D^2 Z_o}{k}(1 - \exp(-z/D)) \quad (2)$$

where k is the thermal conductivity of the crust (~2.5 W m^{-1} $°C^{-1}$) (e.g., Lachenbruch, 1970). The first term on the right hand side is the contribution of conduction through the lithosphere, the second term being the effect of radiogenic heating.

Although $q_r = Z_o D$ (q_r being the radiogenic contribution to surface heat flow q_s; i.e., $q_s = q_r + q_o$) can be estimated for western Turkey, as above, neither Z_o nor D are well-constrained. Nonetheless, using Eq. (2) one can predict that in this region the depth of the base of the brittle layer, z_b, corresponding to a temperature of ~350 °C, is ~10–14 km (taking D=2.5 km and Z_o=22 μW m^{-3} would give z_b ~10.3 km, whereas taking D=14 km and Z_o=3 μW m^{-3} would give z_b ~13.5 km). The depth limit of seismicity independently suggests a relatively shallow base of the brittle layer, ~10 km deep (e.g., Jackson and McKenzie, 1988). Saunders et al. (1998) also inferred that the seismic S-wave velocity in the Kula area of western Turkey (Fig. 2) decreases below a depth of 13 km, providing a third estimate of z_b.

In general, rates of surface processes also affect the geothermal gradient in the continental lithosphere. It is well-known (e.g., Stüwe et al., 1994; Westaway, 2002a) that if crust has experienced denudation at a constant rate U for long enough for a steady-state condition to have developed, with constant temperatures T_o at the Earth's surface and T_1 at a fixed depth H, then temperature T varies with depth z as:

$$\frac{T - T_o}{T_1 - T_o}(1 - \exp(-UH/\kappa)) = 1 - \exp(-Uz/\kappa). \quad (3)$$

where κ is the thermal diffusivity of the material. The magnitude of the perturbation to the geotherm caused by denudation can be expressed using the dimensionless parameter Pe, the denudational Péclet number, which can be written as:

$$Pe \equiv \frac{UH}{2\kappa} \quad (4)$$

(e.g., Westaway, 2002a). Pe quantifies the relative importance of advection and conduction in transferring heat: when $Pe \gg 1$, advection predominates; when $Pe \ll 1$, conduction predominates.

This choice of a fixed temperature boundary condition at the base of the model is to address two situations that are each of geological significance. The first (cf. Stüwe et al., 1994) is where the heat flux through the lithosphere is determined by the temperature at its base, which is fixed due to the effect of convection in the underlying asthenosphere. The second (cf. Westaway, 2002a) is where the temperature near the base of the continental crust is held constant (or near constant), because the crust is in (or near) a steady state in which isostatic compensation of erosion occurs by inflow of an equivalent layer thickness of lower crust (cf. Westaway, 1994a, 2004c). This inflow will be concentrated near the base of the crust (cf. Westaway, 1998, 2002b) and, since it is likely to involve material that is at a similar temperature to that which is already present at this depth, is unlikely to significantly affect the temperature at this depth.

Both radiogenic heating and steady-state denudation will result in convex-upward geotherms. As Westaway (2002a) noted, both effects can produce similar geotherms, there being effectively a trade-off between the parameters U and Z_o. Indeed, for the special case where

$$Pe = \frac{H}{2D} \quad (5)$$

this trade-off is exact and identical geotherms can result from different combinations of values of U and Z_o.

Estimation of present-day geotherms in western Turkey or other continental regions is further complicated by the fact that it is unlikely that present-day denudation rates have persisted for long enough for the steady-state regime specified in Eq. (3) to exist. This is because rates of erosion in many regions increased at the end of the Middle Pliocene (~3 Ma), as a result of climate deterioration accompanying the earliest large-scale Northern-Hemisphere glaciation, then again in the late Early Pleistocene (~0.9 Ma) when the climate experienced further deterioration during cold stages following the onset of ~100 ka climate cyclicity (e.g., Westaway, 2001, 2002a,b,c). Insufficient time has elapsed since these changes for steady-state conditions to have been re-established; indeed, the widespread occurrence worldwide of regional-scale 'epeirogenic' vertical crustal motions, revealed by abundant sedimentary and geomorphological evidence, is thought to reflect this departure from steady-state conditions (e.g., Westaway, 2001, 2002b,c, 2004c). In particular, quantitative modelling of vertical crustal motions in western Turkey by Westaway et al. (2004) suggests strongly that the continental crust in this region is not at present in a thermal steady state.

The crustal thickness in the vicinity of Kula has been determined as 30 ± 1 km from detailed studies of seismic wave propagation (Saunders et al., 1998). Using the same range of values as above (for Z_o and D) places the base of the lithosphere (at a temperature of ~1400 °C) at a depth of ~53–59 km, implying that the mantle lithosphere in this region is <~30 km thick (cf. Ilkışık, 1995). Taking account of the expected perturbation to the geotherm caused by the regional erosion that typefies western Turkey at present (e.g., Westaway et al., 2004), the base of the lithosphere may be expected somewhat deeper that these simple calculations predict (cf. Westaway, 2002a). The present study will thus consider 60 km to be a representative value for the lithosphere thickness in this region, although calculations will also be made for a thicker nominal value of 75 km.

As was briefly noted by Westaway et al. (2005), the simplest approach to investigating the thermal effect of any Cenozoic flat subduction beneath western Turkey would be to only consider the direct consequences of the addition and subsequent removal of a second layer of lithosphere. This process can be investigated using the diffusion equation for vertical heat flow through the lithosphere:

$$\frac{\partial T}{\partial t} = \kappa \frac{\partial^2 T}{\partial z^2}. \tag{6}$$

At time $t=0$, a second layer of thickness L is introduced below the original model lithosphere, which for simplicity is also assumed to have thickness L. Both layers of model lithosphere are assumed to initially have a uniform geothermal gradient, with (again for simplicity) a temperature of 0 °C at the top and T_o, the (constant) asthenospheric temperature, at the base. At time $t=0$, the boundary condition for solution to (6) is thus:

$$T(t=0,z) = T_o z/L \quad (0 \le z < L) \tag{7a}$$

$$T(t=0,z) = T_o(z-L)/L \quad (L \le z \le 2L). \tag{7b}$$

If the second layer remains indefinitely, the geothermal gradient will tend to a uniform limit; thus:

$$T(t \rightarrow \infty, z) = T_o z/(2L). \tag{8}$$

The temperature is also fixed at the Earth's surface and the base of the lower layer of model lithosphere:

$$T(t, z=0) = 0 \tag{9a}$$

$$T(t, z=2L) = T_o \tag{9b}$$

Eq. (6) can be solved subject to the boundary conditions (7), (8) and (9), using a standard method (e.g., Carslaw and Jaeger, 1959, pp. 99–100), to give:

$$T(t,z) = \frac{T_o z}{2L} + \frac{T_o}{\pi} \sum_{n=1}^{\infty} \frac{(-1)^{n+1}}{n} \sin\left(\frac{n\pi z}{L}\right) \times \exp\left(-\frac{n^2\pi^2\kappa t}{L^2}\right). \tag{10}$$

If at a later time t_o the second layer of lithosphere is removed, the thermal state of the remaining layer will gradually recover. Its subsequent development can be solved using the same technique, with boundary conditions for $t \ge t_o$:

$$T(t, z=0) = 0 \tag{11a}$$

$$T(t, z=L) = T_o \tag{11b}$$

$$T(t \rightarrow \infty, z) = T_o z/L \tag{11c}$$

and, from Eq. (10),

$$T(t=t_o,z) = \frac{T_o z}{2L} + \frac{T_o}{\pi} \sum_{n=1}^{\infty} \frac{(-1)^{n+1}}{n} \sin\left(\frac{n\pi z}{L}\right) \times \exp\left(-\frac{n^2\pi^2\kappa t_o}{L^2}\right). \tag{12}$$

The solution for $t > t_o$ is:

$$T(t,z) = \frac{T_o z}{L} + \frac{T_o}{\pi} \sum_{n=1}^{\infty} \frac{(-1)^{n}}{n} \left(1 - \exp\left(-\frac{n^2\pi^2\kappa t_o}{L^2}\right)\right) \times \sin\left(\frac{n\pi z}{L}\right) \exp\left(-\frac{n^2\pi^2\kappa (t-t_o)}{L^2}\right). \tag{13}$$

Any satisfactory thermal model for this study region must be able to predict significant cooling of the crust as a result of mid-Tertiary flat subduction (in order to explain the available thermochronologic data; cf. Ring et al., 2003; Fig. 3) and also be consistent with the present regime of high heat flow (e.g., Ilkışık, 1995). If the above calculations can account for both these aspects, the effort involved in developing the more complex theory necessary to model denudation in the presence of flat subduction becomes worthwhile.

To test this, Fig. 4(a)–(d) illustrates sequences of model geotherms calculated assuming that flat subduction occurred during 28–16 Ma (parts a and b) and during 40–16 Ma (parts c and d) (i.e., using Eq. (10) before 16 Ma and Eq. (13) from then to the present day). It is evident that the associated temperature fluctuations are rather complex. Juxtaposition of the underlying layer of lithosphere causes rapid cooling of the

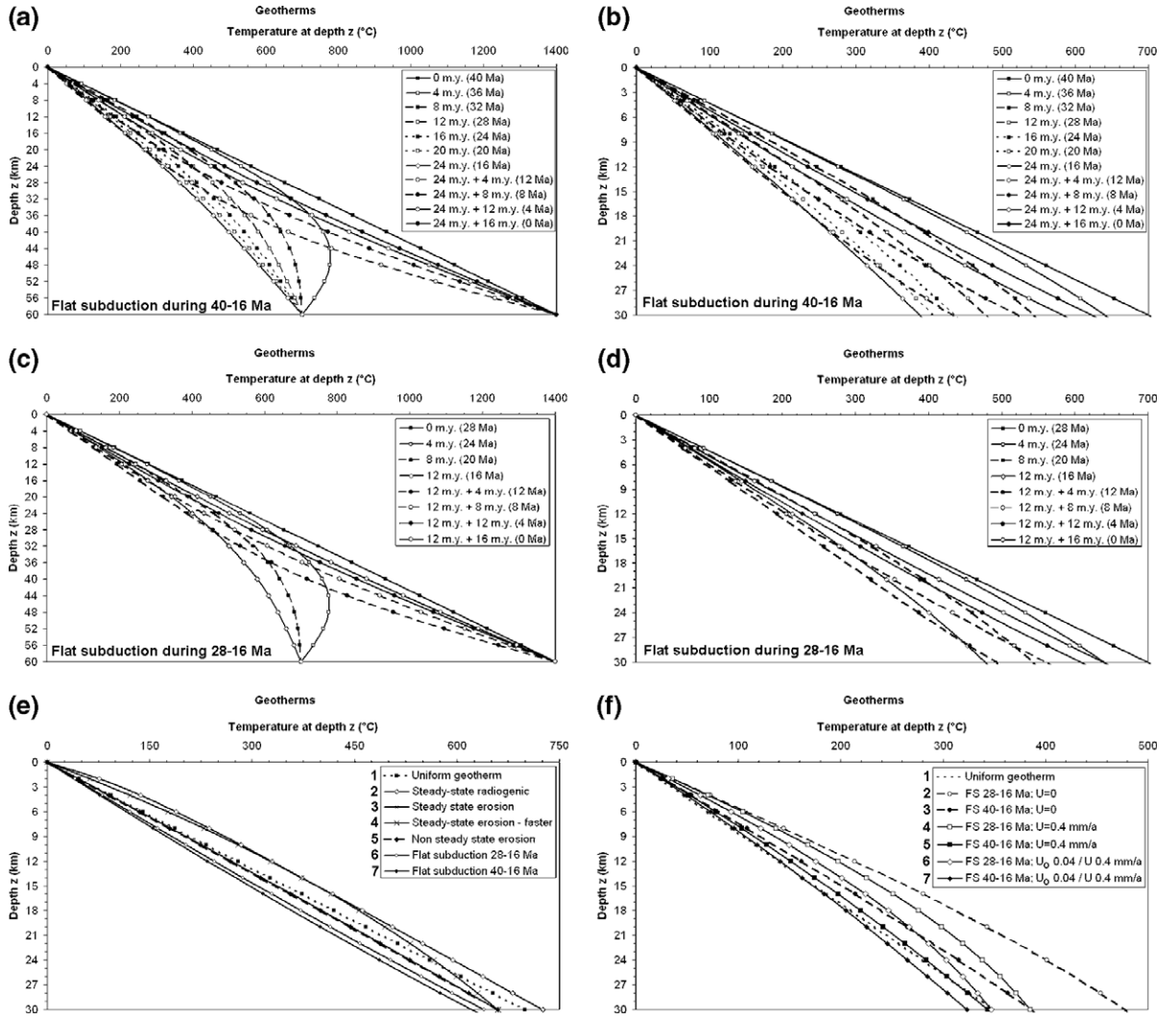

Fig. 4. (a) Model geotherms calculated at 4 million year intervals using Eqs. (10) and (13) for T_a=1400 °C, L=60 km and κ=1.2 mm s^{-1}, for a region affected by flat subduction during 40–16 Ma. (b) Enlargement of the upper part of (a) to show the model crust ($z \leq 30$ km) in more detail. (c) Same as (a) except flat subduction is inferred to have occurred during 28–16 Ma. (d) Enlargement of the upper part of (c) to show the model crust ($z \leq 30$ km) in more detail. (e) Seven different present-day geotherms, each calculated according to a different set of assumptions as described in the text. (f) Seven different possible geotherms for 16 Ma, each calculated as follows. Geotherm 1 has a uniform geothermal gradient of 1400 °C/120 km or 11.67 °C km^{-1}. Geotherms 2 and 3 assume no erosion, with flat subduction 28–16 and 40–16 Ma, with the same set of parameter values as curves 6 and 7 in (e). Geotherms 4 and 5 assume erosion at a constant rate of erosion of 0.4 mm a^{-1}, with the same durations of flat subduction as curves 2 and 3; they use Eq. (29) with boundary condition (22) as for Fig. 5(b). Geotherms 6 and 7 assume that the erosion increased tenfold from 0.04 to 0.4 mm a^{-1} at the start of flat subduction, which involved the same durations as for curves 2 and 3; they use Eq. (33) with boundary condition (22) as for Fig. 5(c).

upper layer, creating for a time an inverted geotherm in the lower part of this upper layer. This pulse of cooling subsequently diffuses upward through the lithosphere. After flat subduction ends, the remaining lower lithosphere becomes rapidly heated, but its upper part continues to cool for a time until the pulse of reheating diffuses to shallower depths. It is thus estimated (Fig. 4(a), (b)) that in a model region with 60 km thick lithosphere where flat subduction persisted from 40 to 16 Ma, the temperature at 16 km depth cooled from an initial 373.3 °C at 40 Ma to 214.1 °C at 16 Ma. It then continued to cool, reaching a minimum of 208.8 °C at 13.5 Ma, before recovering to 315.9 °C at the present-day. In a model region where flat subduction persisted from 28 to 16 Ma (Fig. 4(c), (d)), the temperature at 16 km depth cooled from the same initial value to 257.3 °C

at 16 Ma and has since recovered to 328.8 °C. These data thus suggest that flat subduction is indeed capable of having significantly cooled the lithosphere of western Turkey in mid-Tertiary times, and that—even if it ended as late as the early Middle Miocene—sufficient time has since elapsed for this lithosphere to have almost recovered to its original thermal regime. Both this predicted rapid cooling and the subsequent rapid heating, ensuring that this lithosphere has little long-term thermal 'memory' of past events, are of course consequences of assuming that it is thin; the basis for assigning the lithosphere beneath western Turkey a nominal 60 km thickness was set out earlier.

Fig. 4(e) compares these predicted geotherms, calculated for the present day for flat subduction followed by reheating, with other calculations. Geotherm 1 is for a uniform geothermal gradient of 1400 °C/60 km or 23.33 °C km^{-1}. Geotherm 2 is a strongly convex-upward geotherm calculated assuming a steady-state regime in response to radiogenic heating, calculated using Eq. (2) for $Y_o = 18.3$ μW m^{-3} and $D = 3$ km. Geotherm 3, much less strongly convex-upward, is calculated using Eq. (3)—for a steady-state thermal regime governed by denudation—with a present-day erosion rate U of 0.1 mm a^{-1}, with $H = 30$ km and $T_1 = 660$ °C. Such an erosion rate is typical of time-averaged conditions in much of western Turkey, as discussed by Westaway (1994b) and Westaway et al. (2004). H is set here to 30 km, the crustal thickness, not the lithosphere thickness, because the isostatic compensation of the loss of mass caused by the erosion in this region is inferred to be by inflow of lower crust, which has the effect of maintaining a roughly constant Moho temperature (Westaway et al., 2004). The Moho temperature of 660 °C that is used is also consistent with the rheological modelling by Westaway et al. (2004). Geotherm 4 is calculated for a steady-state regime governed by erosion, using the same parameters as for geotherm 3 except U has been increased ten-fold to 1 mm a^{-1}. This is to demonstrate the point that with an appropriate choice of parameter values, a geotherm calculated on this basis can roughly resemble one calculated for radiogenic heating (cf. Westaway, 2002a). However, geotherm 4 cannot precisely match geotherm 2 throughout the model crust, because no attempt has been made to impose the condition that $Pe = H/2D$ (Eq. (5)); $H/2D$ is 30/6 or 5, whereas, from Eq. (4), Pe is ~0.4 for an erosion rate of 1 mm a^{-1}. Geotherm 5 is calculated for the non-steady-state thermal regime expected using Eq. (B19) of Westaway (2002a), 3.1 million years after a change from sedimentation at 0.025 mm a^{-1} to erosion at 0.1 mm a^{-1}, assuming as before that a fixed temperature of 660 °C is maintained at 30 km depth. These parameters are appropriate for the Kula region of western Turkey; the 3.1 Ma start of erosion and the sedimentation rate before this time (for deposition of a maximum thickness of 100 m of lacustrine limestone of the Ulubey Formation, during ~7 to ~3 Ma) are explained by Westaway et al. (2004). This predicted curve differs very little from geotherm 4 for steady-state conditions with the same present-day erosion rate. Geotherms 6 and 7 are calculated using the same parameters as for Fig. 4(a)–(d), for flat subduction during 28–16 Ma or during 40–16 Ma.

It is evident that there is considerable variability between these calculated geotherms. However, the geotherms calculated for erosion at the present-day rate (3 and 4) are quite similar to those calculated for conditions following flat subduction (6 and 7). This confirms the earlier conclusion that the thermal regime in the crust has virtually recovered following any mid-Tertiary flat subduction. It is also evident that all these geotherms significantly underestimate the temperature in the shallow part of the crust given the expected magnitude of radiogenic heating. This suggests that more complex calculations, incorporating effects of erosion and/or radiogenic heating into the thermal response to flat subduction, are worthwhile.

3. Thermal histories including denudation during flat subduction

Denudation causes the upper part of the crust to move vertically relative to a fixed reference frame. To obtain the temperature T within material moving relative to a reference frame (defined using Cartesian x, y, z coordinates with z downward and $z = 0$ at the Earth's surface) requires the solution of the advective diffusion equation

$$\kappa \nabla^2 T = \boldsymbol{v} \cdot \nabla T + \partial T / \partial t \qquad (14)$$

where κ is the thermal diffusivity of the material and $\boldsymbol{v}(x, y, z)$ is its velocity relative to the reference frame. If denudation removes material from the horizontal Earth's surface at rate U, then T only varies vertically and $v_z = -U$ near $z = 0$. Also, for any steady state solution $\partial T / \partial t = 0$. The simplest solution relevant to geothermal studies is for a layer of thickness H with surfaces at constant temperatures: $T(z = 0) = T_o$ ($T_o = 0$ °C) and $T(z = H) = T_1$, T_o and T_1 being constants, and is

$$T(z) = C_1 + C_2 \exp(-Uz/\kappa) \qquad (15)$$

where C_1 and C_2 are constants. Matching the specified boundary conditions determines C_1 and C_2, such that

Eq. (15) can be written (e.g., Stüwe et al., 1994; Westaway, 2002a) as Eq. (3), as already stated.

To calculate the distribution of temperature T as a function of depth z and time t in the continental crust, following the start of flat subduction, as lithosphere of thickness L becomes underlain by a second layer of lithosphere, also of thickness L, in the presence of denudation at rate U, requires solution of Eq. (14) in the form

$$\kappa\frac{\partial^2 T}{\partial z^2}+U\frac{\partial T}{\partial z}=\frac{\partial T}{\partial t}, \tag{16}$$

subject to boundary conditions

$$T(z=0,t)=0, \tag{17}$$

$$T(z=2L,t)=T_a, \tag{18}$$

$$T(z,t=0)=T_a\frac{1-\exp(-Uz/\kappa)}{1-\exp(-UL/\kappa)}=T_a\frac{1-\exp(-Uz/\kappa)}{R}\quad(0\le z\le L), \tag{19}$$

and

$$T(z,t\rightarrow\infty)=T_a\frac{1-\exp(-Uz/\kappa)}{1-\exp(-2UL/\kappa)}=T_a\frac{1-\exp(-Uz/\kappa)}{S}\quad(0\le z\le 2L). \tag{20}$$

Conditions (17) and (18) state the requirement that the temperature is fixed at zero at the Earth's surface and at the start is the asthenosphere temperature T_a at depth L. Condition (19) states that immediately before the start of flat subduction the geotherm in the upper layer of lithosphere is the steady-state regime for denudation at a rate U (Eq. (3)). Condition (20) states that ultimately the geotherm will tend to that expected for denudation at rate U in lithosphere of thickness $2L$. Within the continental crustal column, denudation will cause material to advect upwards, the loss of material from the surface being typically balanced by inflow of lower crust from the sides (e.g., Westaway, 1994a,b, 2002a). The assumption of upward advection at a constant rate U down to this level is thus justified. However, the material forming the underlying mantle lithosphere and that of the second layer of lithosphere will not be advecting upwards. The solutions presented thus contain an approximation. Nonetheless, as Westaway (2002a) noted, in such modelling the conditions in the upper layer of crust are relatively insensitive to details of conditions assumed at much greater depth. Furthermore, as already noted, under the conditions deduced for western Turkey, the denudational Péclet number (Eq. (5)) is relatively low, so upward advection of material only accounts for a fraction of the calculated heat transport.

One also requires an initial temperature distribution in the lower layer of lithosphere (i.e., specify $T(z,t=0)$ for $L\le z\le 2L$). Two end-member possibilities will be considered. The first, appropriate if this layer has already spent such a long time beneath the overlying layer elsewhere that it has already heated up to the asthenosphere temperature T_a, is

$$T(z,t=0)=T_a\qquad(L\le z\le 2L). \tag{21}$$

The second is a uniform initial geotherm (consistent, for instance, with very old oceanic lithosphere that has only just been juxtaposed beneath the overlying layer):

$$T(z,t=0)=T_a(z-L)/L\qquad(L\le z\le 2L). \tag{22}$$

The general procedure for solving Eq. (16), with a similar set of boundary conditions, was thoroughly explained by Westaway (2002a); this solution is

$$T(z,t)=(T_a/S)(1-\exp(-Uz/\kappa))+\sum_{n=1}^{\infty}B_n\sin(n\pi z/(2L))\exp(-Uz/(2\kappa))\times\exp\left(-\left(U^2/(4\kappa)+n^2\pi^2\kappa/\left(4L^2\right)\right)t\right). \tag{23}$$

The coefficients B_n can be determined using Fourier analysis for each set of boundary conditions at $t=0$.

With Eqs. (19) and (21) one obtains

$$B_n=\frac{A_n+C_n+D_n}{1+n^2\pi^2/Y^2}, \tag{24}$$

where

$$Y\equiv LU/\kappa, \tag{25}$$

$$A_n=\frac{4n(-1^n)\pi}{SY^2}T_a\sinh(Y), \tag{26}$$

$$C_n=(4T_a/(RY))\sin(n\pi/2)\cosh(Y/2)-\left(4n\pi T_a/\left(RY^2\right)\right)\cos(n\pi/2)\sinh(Y/2),\ \text{and} \tag{27}$$

$$D_n=(2T_a/(Y))\sin(n\pi/2)\exp(Y/2)-\left(2n\pi T_a/Y^2\right)\times(-1^n\exp(Y)-\cos(n\pi/2)\exp(Y/2)). \tag{28}$$

In this instance, with $H=2L$, the Péclet number Pe (Eq. (4)) will equal Y in Eq. (25). The cooling history solutions for western Turkey in Fig. 3 thus have $Pe\sim 1$, so both advection and conduction are significant.

With Eqs. (19) and (22) as the boundary conditions one instead obtains

$$B_n = \frac{A_n + C_n + E_n + F_n}{1 + n^2\pi^2/Y^2}, \tag{29}$$

where A_n and C_n are as before (Eqs. (26) and (27)),

$$E_n = -D_n\left(1 + \frac{4Y}{Y^2 + n^2\pi^2}\right), \tag{30}$$

$$F_n = -(2T_a/Y)\sin(n\pi/2)\exp(Y/2) - \left(2n\pi T_a/Y^2\right) \times (2(-1^n)\exp(Y) - \exp(Y/2)(\cos(n\pi/2) + \sin(n\pi/2))). \tag{31}$$

No attempt is made here to calculate the heating effect that occurs in the model crust that continues to experience denudation after the ending of flat subduction. This is, first, because earlier experience for the simpler case of flat subduction with no denudation (Eq. (13)) suggests that the algebra with denudation included will be dauntingly complex. Second, for the localities of interest in western Turkey, by the time flat subduction is considered likely to have ended the points that have yielded thermochronologic data sets are expected to already be at such shallow depths that there is no time for this heating effect to reach them.

Likewise, no attempt is made at this stage to calculate the combined effects on the geotherm of flat subduction, denudation, and radiogenic heating, all together. This is, first, because of the anticipated algebraic complexity of these solutions, which can be inferred by inspection of the solutions above for simultaneous flat subduction and denudation and those by Westaway (2002a) for simultaneous radiogenic heating and denudation. Second, the existing literature on conditions in western Turkey in the Early Tertiary (e.g., Whitney and Bozkurt, 2002) indicates at least ~20 km of subsequent denudation. This is much greater than the likely present-day local value of D, the depth scale for radiogenic heating, as discussed earlier. This means that the part of the rock column that is now at shallow crustal depths and is inferred to be significantly enriched in radioactive heat-producing elements was probably much more depleted in these elements in the Early Tertiary, this inferred enrichment presumably relating to processes that have occurred on the intervening time scale (e.g., hydrothermal circulation associated with flat subduction and/or crustal shortening and/or crustal extension). Conversely, the magnitude of contemporaneous radiogenic heating in the part of the rock column that formed the shallow crust in western Turkey in the Early Tertiary is unknown. No basis even for making a crude estimate exists: for instance, it is unknown whether it is likely that the atoms of the radiogenic heat producing elements that were present in the shallow crust at the time have since been removed by erosion, being since replaced by a different set of atoms from deeper in the Earth's interior, or whether the same set of atoms keeps being transported downward through the crustal rock column by groundwater circulation as this rock column becomes progressively eroded. Third, previous experience (e.g., Westaway, 2002a, and Fig 4(e) and the associated discussion in the present text) indicates that radiogenic heating and erosion may result in similar geotherms, with a trade-off between the parameters Z_o and U. It follows that to neglect radiogenic heating will mean that solutions are fitted using values of the erosion rate U that overestimate the true values. The estimates of U used for each of the predicted geotherms that incorporate erosion are thus upper bounds, which would exceed the true values appropriate for the Early Tertiary in this study region if contemporaneous radiogenic heating of the crust was significant.

Fig. 5(a) and (b) indicate how the predicted geotherm varies over time after the start of flat subduction, for solutions of the forms of Eqs. (24) and (29). It is evident from Fig. 5(a) that introduction of a second layer of initially very hot lithosphere causes only minimal cooling at crustal depths on time-scales of interest. However, introduction of a second layer of cold lithosphere promptly causes dramatic perturbations to the geotherm at crustal depths in the original upper layer of lithosphere. This is consistent with what is observed at the start of flat subduction of cold oceanic lithosphere in the absence of denudation (Fig. 4(a)–(d)). Fig. 4(f) shows a set of possible predicted geotherms calculated for western Turkey at the nominal 16 Ma end of flat subduction that was used earlier.

These time-dependent geotherms can be used to construct model cooling histories for comparison with observations in western Turkey (as in Fig. 3). It is thus evident that a geotherm of the form in Fig. 5(a) cannot generate the observed strongly non-uniform cooling history, but instead approximates the near-uniform cooling history expected in the absence of flat subduction. However, geotherms of the form of Fig. 5(b) can match the observations of rapid cooling before ~20 Ma. This test suggests that flat subduction ended no earlier than ~20 Ma, in the Early Miocene, although as already noted, it cannot constrain how

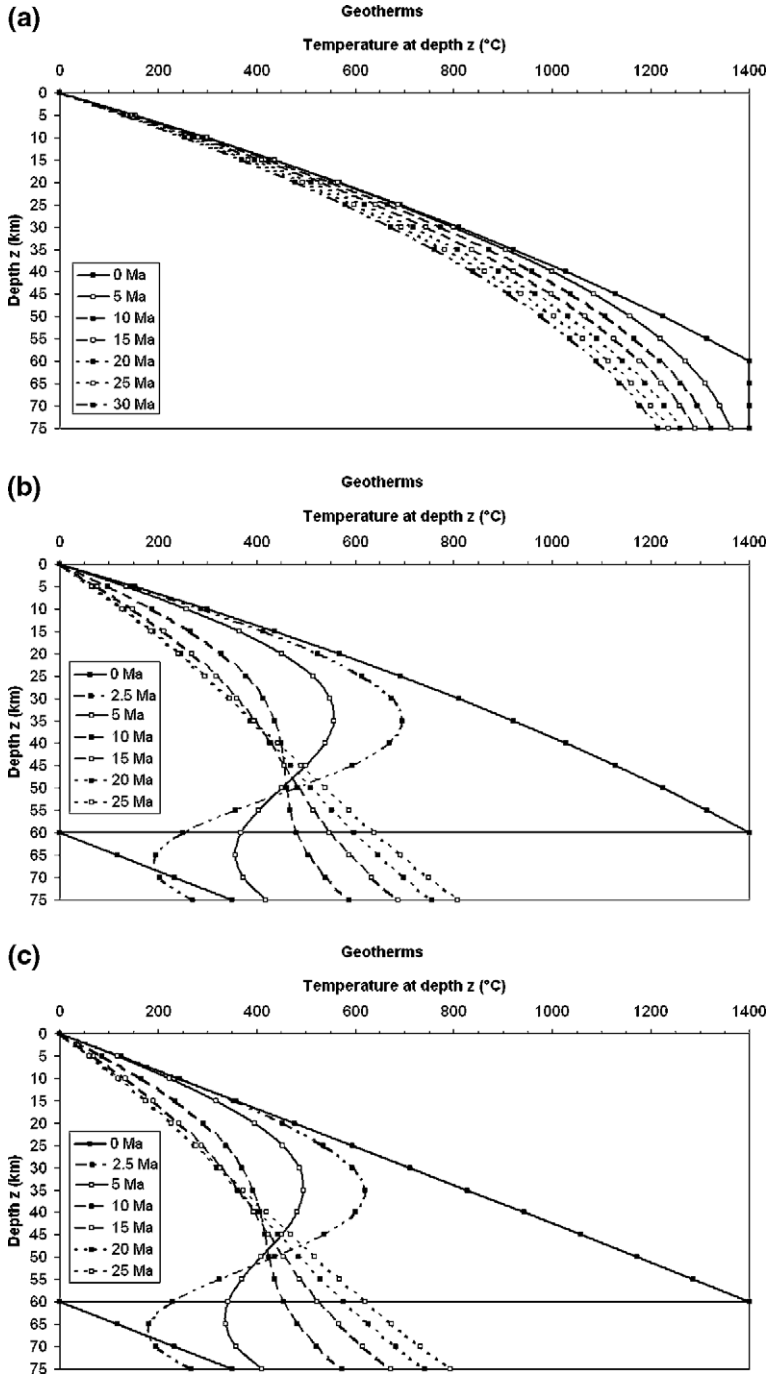

Fig. 5. Model geotherms predicted for $L=60$ km, $U=0.4$ mm a^{-1}, $T_a=1400$ °C, and $\kappa=1.2$ mm^2 s^{-1} (i.e., $Y=Pe=0.63$). (a) Based on Eq. (24), using boundary condition (21) (i.e., assuming that flat subduction caused the continental lithosphere of western Turkey to be underlain by a second 60 km thick layer of hot lithosphere at a constant temperature of 1400 °C). (b) Based on Eq. (29), using boundary condition (22). (i.e., assuming that flat subduction caused western Turkey to be underlain by a second 60 km thick layer of cold lithosphere across which the temperature initially increased linearly from 0 to 1400 °C). (c) Based on Eq. (33), using boundary condition (22), also with $U_o=0.04$ mm a^{-1} (i.e., assuming again that flat subduction caused western Turkey to be underlain by a second 60 km thick layer of cold lithosphere across which the temperature initially increased linearly from 0 to 1400 °C, but that the start of flat subduction also corresponded with a ten-fold increase in typical erosion rates). See text for discussion.

much later it did end. The model solutions, for relatively thin lithosphere ($L=60$ km), are consistent with a start of flat subduction at ~35–40 Ma, in the Late Eocene or Early Oligocene. Alternative solutions (not shown) with thicker lithosphere would require an earlier start of flat subduction. However, considerations of regional tectonic evolution (cf. Garfunkel, 2004; see also below) make it unlikely that this process began before the Middle Eocene (~45 Ma).

A possible refinement (discussed in more detail below) is to infer that the onset of flat subduction will cause deformation of the overlying continental crust leading to a general increase in erosion rates. If so, the thermal response to this increase, from U_o to U (cf. Westaway, 2002a), will be superimposed on that due to flat subduction. To implement this change the boundary condition in Eq. (19) is replaced by:

$$T(z,t=0) = T_a \frac{1-\exp(-U_o z/\kappa)}{1-\exp(-U_o L/\kappa)} = T_a \frac{1-\exp(-U_o z/\kappa)}{R_o} \quad (0 \le z \le L). \quad (32)$$

The resulting solution (assuming the condition specified by (22) and (32) at $t=0$) is:

$$B_n = \frac{A_n + E_n + F_n + G_n}{1 + n^2\pi^2/Y^2} - \frac{J_n}{1 + n^2\pi^2/Z^2}, \quad (33)$$

with

$$G_n = (2T_a/(R_o Y))\sin(n\pi/2)\exp(Y/2) + \left(2n\pi T_a/\left(R_o Y^2\right)\right)(1-\cos(n\pi/2)\exp(Y/2)), \quad (34)$$

$$J_n = (2T_a/(R_o Z))\sin(n\pi/2)\exp(Z/2) + \left(2n\pi T_a/\left(R_o Z^2\right)\right)(1-\cos(n\pi/2)\exp(Z/2)), \quad (35)$$

and

$$Z \equiv L(U-2U_o)/\kappa. \quad (36)$$

4. Cooling histories in western Turkey

The Menderes Massif can be conveniently divided into three parts: the Çine Massif south of the BMFZ, the Gördes Massif north of the AFZ, and the Central Massif in between (Fig. 2). Representative localities will be considered from each, using the thermochronologic dataset of Ring et al. (2003). To facilitate comparison with their work, comparable closure temperatures of 425 ± 25 and 350 ± 25 °C are assumed for argon retention in muscovite and biotite, and 260 ± 20 and 110 ± 10 °C for fission-track annealing in zircon and apatite. In contrast, a closure temperature of 550 ± 25 °C is assumed for argon retention in amphibole, rather than the much lower value used by Ring et al. (2003). This latter value is justified (cf. McDougall and Harrison, 1999, p. 159) given the large grain size of their samples (250–500 μm) and the order-of-magnitude of cooling rates (tens of °C/Ma) expected in this region around the time of closure.

The start of flat subduction is expected to be progressively later as one moves northward across the study region, it being determined by the position of the leading edge of this slab as it moves northward beneath the overlying continental lithosphere. Given the approximation already made that the equations used to determine cooling histories ignore horizontal components of heat flow, this northward progression can be represented simply by varying the start time of flat subduction between localities.

4.1. The Çine Massif

Fig. 3(a) shows data and a predicted cooling history for the southern Çine Massif around Milas (Fig. 2). This is a region with no significant young extension; cooling histories can thus reasonably be attributed to processes occurring beforehand. Being close to the southern margin of the Menderes Massif, near its contact with the Lycian Nappes farther south, the cooling history of this region has previously been attributed to "tectonic denudation" as a result of large-scale low-angle normal slip on a hypothetical south-dipping "Lycian detachment", which has supposedly translated the Lycian Nappes southward in its hanging-wall and thus unroofed this part of the Menderes Massif in its footwall (see Ring et al., 2003, and many other studies; Fig. 2), exhuming the sites that have yielded the thermochronologic evidence from mid-crustal depths to the Earth's surface. This hypothetical structure has been considered active during the Late Oligocene to Early Miocene from the phase of rapid cooling observed at this time (Fig. 3(a)).

The modelled cooling history indeed suggests exhumation from mid-crustal depths, but as a result of erosion at a typical mid-Cenozoic rate of ~0.4 mm a^{-1}, accompanied by the cooling effect of flat subduction. As already noted, this flat subduction is modelled as beginning to affect this region at ~40–35 Ma (Fig.

3(a), (e)), and continued until at least ~20 Ma, by which time the study sites had cooled to below the ~110 °C closure temperature for fission-track annealing in apatite, even though they are presumed to have still been at substantial depths (almost ~10 km). At this time the predicted geothermal gradient, averaged across the upper 10 km of crust, was only ~13 °C km^{-1}. As already noted, the subsequent heating effect following the ending of flat subduction has not been modelled directly (but see Fig. 4). It has evidently contributed to re-establishing this region's high present-day geothermal gradient, consistent with heat-flow studies (e.g., Ilkışık, 1995).

Located within the Çine Massif are several sedimentary basins, for instance the Yatağan Basin (Fig. 2) and the Kale-Tavas Basin, whose SW part is in the Kale-Göktepe area (Fig. 1). The Yatağan Basin contains a Middle Miocene terrestrial sequence, not thought to be extension-related, which is well-dated due to interbedded volcanism (e.g., Besang et al., 1977; Becker-Platen et al., 1977; Westaway et al., 2005). Fission-track dates for samples T90 and T93 from adjacent sites (Fig. 2), indicate rapid cooling immediately before the Middle Miocene (Fig. 3(a), (e)). It is suggested that this marked the erosion of former cover of the Lycian Nappes from this area, exhuming an irregular land surface in the metamorphic basement, in which localised topographic lows subsequently acted as depocentres, such as at Yatağan. Farther east, the ~60 km long NE–SW-trending Kale-Tavas basin contains Oligocene to Early Miocene shallow marine sediment overlain by a late Middle Miocene to Pliocene terrestrial sequence (e.g., Gökçen, 1979, 1982; Hakyemez, 1989; Yılmaz et al., 2000; Akgün and Sözbilir, 2001). Its Oligocene to Early Miocene sequence, the Akçay Group or "Denizli molasse", has been accepted as not extension-related (e.g., Akgün and Sözbilir, 2001). The overlying terrestrial sequence (the Muğla Group) has been considered extension-related (cf. Hakyemez, 1989; Akgün and Sözbilir, 2001). However, no evidence of active normal faulting has been presented, the deduction that this deposition was extensional was based on coarse clastic input and on inferences that its deposition fell within the time-scale when extension has been thought by the authors to have taken place; both these arguments are now considered weak (cf. Westaway et al., 2005). Despite this uncertainty, it is clear that this sedimentary evidence is incompatible with the phase of Late Oligocene–Early Miocene low-angle normal faulting proposed in this region by Ring et al. (2003) and others.

4.2. The Central Massif

Fig. 3(b) shows thermochronologic data for the central Menderes Massif. This region was regarded by Hetzel et al. (1995a,b) as having been exhumed by many tens of kilometres of "bivergent" extension on a south-dipping normal fault zone associated with the BMFZ and a north-dipping one associated with the AFZ. Although Hetzel et al. (1995a,b) and other studies have inferred that these faults formed with low-angle dips, as already noted this view conflicts with the angular relationships between the dips of normal faults and adjacent sediments (cf. Gessner et al., 2001b). Despite the more limited data, the overall cooling history indicated in this Central Massif is very similar to that in the Çine Massif (Fig. 3(b)); the main difference is that cooling is slightly later, reaching ~260 °C at ~24 Ma instead of ~25–28 Ma. This is consistent with progressive northward migration of the leading edge of a flat subducted slab.

If the cooling in this region was instead the result of extension by low-angle normal faulting, this phase of extension would have been underway in the latest Oligocene/Early Miocene. However, there is no independent evidence for such a timing either in the AFZ or BMFZ. The onsets of extension on these fault zones have been disputed, and these disputes have occupied a vast literature in recent years (see, e.g., Westaway et al., 2004, 2005, for summaries), but this disputed range — based on local sedimentary evidence — spans from the late Early Miocene to early Late Miocene and no further back in time. The dispute hinges on whether all the Miocene sequences in these areas are extension-related or whether their lower parts were deposited — like the Denizli molasse — in localised depocentres that were not extension-related. There is no local sedimentary evidence for latest Oligocene or early Early Miocene extension.

4.3. The footwall of the Alaşehir Fault Zone

The northern margin of the central Menderes Massif abuts the north-facing Alaşehir Fault Zone, which forms the contact between metamorphic basement in its footwall and Neogene sediments in its hanging-wall. The local thermochronologic data indicate progressive cooling until the early Middle Miocene, then a phase of no significant temperature variation until the late Late Miocene (~7 Ma), then subsequent rapid cooling (Fig. 3(c)). The start of this final phase of rapid cooling is dated to 6.68 ± 1.33 Ma, from the closure to argon retention in biotite, determined in this study as the

weighted mean of the dates of two splits of sample GD of Lips et al. (2001). The rocks now exposed in this footwall were thus at ~350 °C at this time, indicating subsequent exhumation from mid-crustal depths. The start of this rapid cooling suggests the start of regional extension; indeed, its timing is consistent with the interpretation by Westaway et al. (2005) from dating of extension-related volcanism, that the present phase of extension began throughout much of western Turkey at ~7 Ma, having been of more limited extent since ~11 Ma (Fig. 1). Like in other localities, the earlier phase of cooling can be explained as a consequence of flat subduction. There is thus no thermochronologic evidence for any extension in this region prior to ~7 Ma.

As already noted, sediments exposed in the hanging-wall of the AFZ date from the late Early Miocene onwards (e.g., Seyitoğlu and Scott, 1996; Koçyiğit et al., 1999; Yılmaz et al., 2000; Bozkurt, 2000, 2002; Seyitoğlu et al., 2002; Bozkurt and Sözbilir, 2004; Purvis and Robertson, 2004). However, there has been no consensus as to which of them are extension-related and which accumulated in an unrelated pre-existing structural depression. The thermochronologic evidence thus now provides a much better indication of the timing of extension on the AFZ than do these controversial sedimentary sequences. In both the AFZ and BMFZ, the switch from extension on the initial set of normal faults to extension on the steeper set of normal faults that is now active seems, from mammalian biostratigraphic evidence (e.g., Ünay and de Bruijn, 1998; Sarıca, 2000) to have occurred in the late Early Pleistocene, possibly because an increase in erosion rates affected the isostatic configuration, causing the maximum principal stress in the vicinity of the AFZ to plunge south, making the initial set of normal faults too severely misaligned relative to the stress field for extension on them to continue (cf. Westaway, 1998).

4.4. The Gördes Massif

Located north of the central Menderes Massif, the exposed metamorphic basement of the Gördes Massif is transected by NE–SW-trending Late Cenozoic terrestrial sedimentary basins (the Gördes, Demirci, Selendi, and Uşak-Güre Basins; Fig. 2). Many studies have debated the possible relationship of these basins to crustal extension, leading to a variety of models. Recently, a consensus has emerged that their sedimentary sequences, which span time from the late Early Miocene onwards, are not extension-related (e.g., Westaway et al., 2003a, 2004, 2005; Purvis and Robertson, 2004). The most obvious evidence in support of this view, obtained from recent fieldwork, is that these sediments lap onto the metamorphic basement at the edges of these basins, with no evidence that these margins were active normal faults during deposition. This view thus supersedes previous interpretations, such as that by Seyitoğlu (1997), but represents a return to how these basins were perceived when first mapped in detail by Ercan et al. (1978).

However, several studies (e.g., Ring et al., 2003; Purvis and Robertson, 2004) have interpreted the upper surface of metamorphic basement beneath these basins as the footwall of a low-angle normal fault that was active at an earlier stage. In such schemes, rocks that overlie this basement, such as inliers of ophiolite from the İzmir-Ankara suture, are interpreted as "riders" of hanging-wall material left overlying the inferred low-angle normal fault plane. An example is shown in Fig. 2 at Değirmenler in the Selendi Basin, but its base is not exposed (e.g., Westaway et al., 2003a, 2004) so such an interpretation is pure conjecture. Elsewhere, where field relationships are clearer, there is no supporting evidence for such an interpretation (cf. Ercan et al., 1978). Ring et al. (2003) deduced rapid cooling in this area in the Early Miocene (Fig. 3(d)) and thus inferred that their "Gördes detachment" was active then. However, this inferred age is contradicted by the age of the basin sediments (cf. Westaway et al., 2004; Purvis and Robertson, 2004). Likewise, the inference by Purvis and Robertson (2004) that this hypothetical "detachment" was active no later than the Late Oligocene is contradicted by the interpretation of cooling ages by Ring et al. (2003).

As Fig. 3(d) makes clear, the interpretation of rapid Early Miocene cooling in this area by Ring et al. (2003) depends on only one sample (93T9), and is dramatically inconsistent with another sample (T68) from a nearby locality (Fig. 2) which, for some reason, they excluded from their interpretation. If one instead adopts sample T68 as representative of this region, the picture that emerges is one of prolonged slow cooling. The somewhat faster net cooling of neighbouring sites (T52, T57 and T59), which are closer to the Gördes Basin, presumably reflects their exhumation from beneath sediments of this basin following recent erosion (cf. Westaway et al., 2004). All these samples were probably already too cold when flat subduction affected this region for any thermal perturbation caused by it to have left any record. The much faster cooling implied by sample 93T9 may reflect some local anomaly, for instance a hot spring (cf. Westaway, 1996) or heating by local Early Miocene volcanism (cf. Purvis and Robertson, 2004). Further study is evidently needed to estab-

lish which existing sample is representative, but in the meantime there is no basis for inferring any low-angle normal faulting in this region.

5. Discussion

The quantitative approach from first principles that has been adopted in this study clearly has its limitations. The principal approximations made have been explained in detail; other related issues are discussed below. As already noted, the calculations assume vertical heat flow in all localities; they thus do not consider local variations such as may have been induced by past juxtaposition of thrust sheets with different thermal histories. Consideration of such variations seems necessary to explain in detail some pressure-temperature path datasets in the Menderes Massif (such as that of Ring et al., 2001), but is beyond the scope of this study. Likewise, no attempt is made to evaluate quantitatively the thermal history of the Menderes Massif throughout its phases of metamorphism. In principle, this could be attempted using existing quantitative solutions such as those of Thompson and England (1984a,b) and England and Thompson (1986), but as these do not consider the thermal effects of flat subduction they are of no help regarding the main subject matter of the present study. The calculations in this study relate only to the Menderes Massif, it being evident that other metamorphic terranes in surrounding regions, such as those in the Cyclades Islands to the west (e.g., Gessner et al., 2001c), the Kazdağ Massif to the north (e.g., Okay and Satır, 2000) and the Kırşehir Massif to the east (e.g., Whitney and Hamilton, 2004) have experienced different thermal and deformational histories.

The reinterpretation proposed in this study suggests that previous schemes involving Cenozoic low-angle normal faulting in western Turkey (e.g., Hetzel et al., 1995a,b; Özer and Sözbilir, 2003; Ring et al., 2003) are a conflation of two unrelated forms of evidence. For two of the four supposed low-angle normal fault systems that have been inferred, the "Lycian detachment" in the south and "Gördes detachment" in the north (Fig. 2), cooling histories due to erosion have been mistaken for cooling histories caused by "tectonic denudation" by low-angle normal faulting. For the other two, the "Kuzey detachment" along the line of the AFZ and the "Güney detachment" along the line of the BMFZ (Fig. 2), extension has only affected the most recent parts of the cooling histories. Although the available thermochronologic data does not yet permit a reliable determination of the start of extension in the BMFZ, the estimate that extension involving steep normal faulting in the AFZ began at ~7 Ma fits a regional scheme by Westaway et al. (2005). Furthermore, angular relationships between dips of sediments and of normal faults indicate that these normal faults formed with steep initial dips, not low-angle dips; they should thus not be considered as examples of detachment faulting, regardless of the timing of their slip.

Fig. 6 suggests a schematic regional model consistent with the above interpretations, also consistent with the overall evolution history of the Eastern Mediterranean region proposed by Garfunkel (2004). In Fig. 6(a), in the Early to Middle Eocene, narrow Mesozoic ocean basins remained in what is now western Turkey. Convergence between the African and Eurasian plates was accommodated by their progressive closure, shown schematically by the northward subduction of the İzmir-Ankara ocean beneath the Pontide continent and of the South Tauride ocean beneath the Bey Dağları continent. Convergence at this time across the Inner Tauride ocean could have been accommodated by thrusting of the Lycian Nappes onto the surrounding continental fragments (cf. Collins and Robertson, 1998; Garfunkel, 2004). In Fig. 6(b), representing the Late Eocene to Oligocene and Early Miocene, progressive northward flat subduction of the oceanic lithosphere of the Eastern Mediterranean ocean basin is depicted beneath all the continental fragments comprising western Turkey. At the same time, material was being eroded from these regions, and the resulting cooling of the lithosphere began to influence its crust, as previously calculated. By analogy with western South America (e.g., Gutscher et al., 2000), a possible reason why this phase of subduction was flat was that the oceanic crust forming the original northern part of the eastern Mediterranean Basin consisted of one or more aseismic ridges, whose relative buoyancy prevented steep subduction. It is of course impossible to test this suggestion, because this crust has since been destroyed, although lateral variations in the geometry of the modern Hellenic slab can also plausibly be related to variations in the composition of the crust being subducted (cf. Laigle et al., 2004).

In addition to cooling the overlying lithosphere, this inferred phase of flat subduction can be deduced to have had two other effects. First (cf. Gutscher et al., 2000), its contact with the upper layer of lithosphere across a wide plate interface can be expected to have imparted horizontal shear tractions on this upper layer of lithosphere, in a sense consistent with causing it to shorten and thicken. As previously noted, the calculation procedure can be modified consistent with the assumption that the start of flat subduction also marked

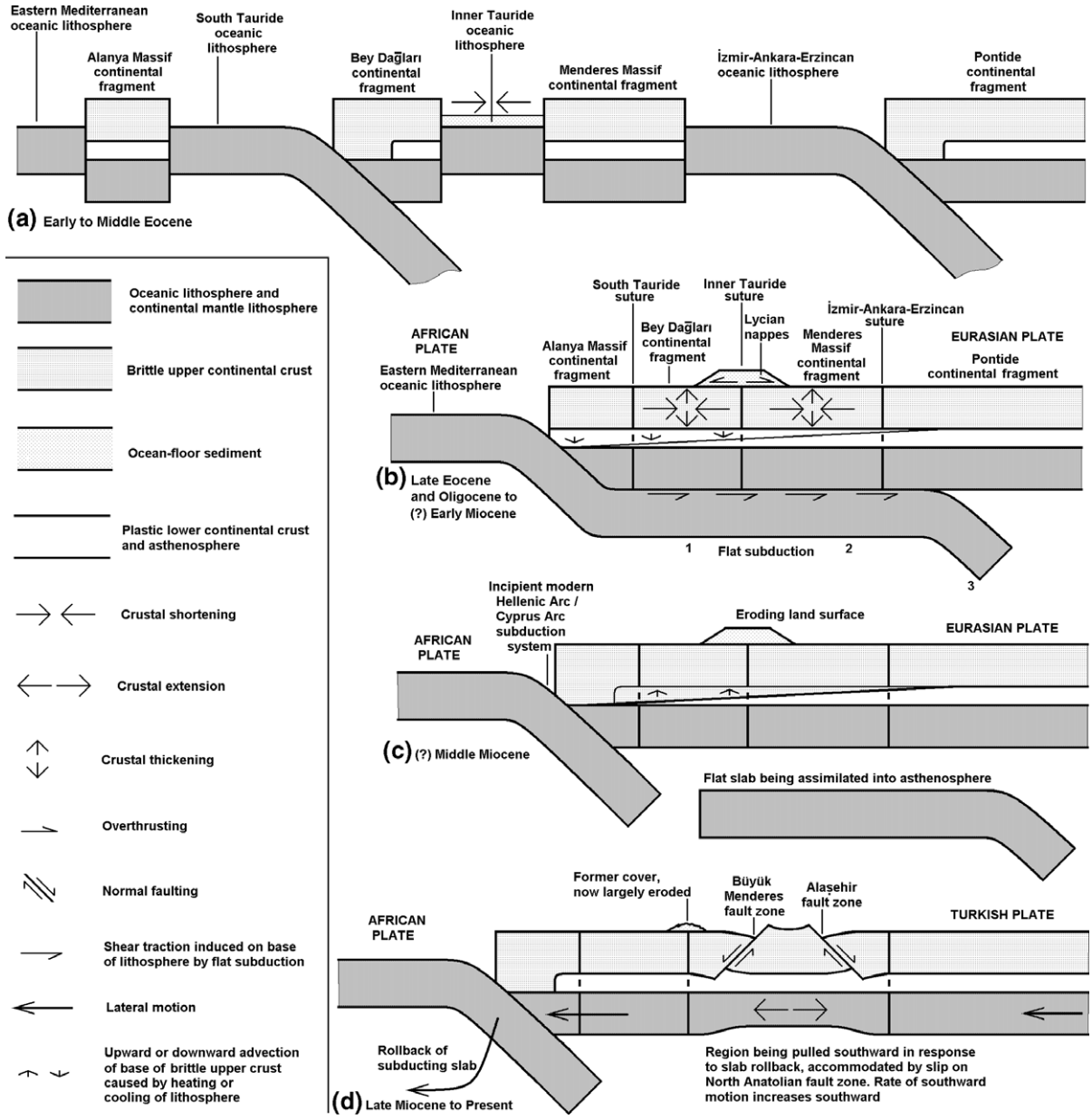

Fig. 6. Schematic regional evolutionary model. (a) In the Early to Middle Eocene. (b) In the Late Eocene and Oligocene to (?) Early Miocene. 1 2 and 3 mark three successive suggested northward limits for the flat slab. (c) In the (?) Middle Miocene. (d) In the Late Miocene to present. See text for discussion.

a general increase in erosion rates, which would be a plausible consequence of such deformation. Fig. 3(e) and (f) show that such a modification can eliminate the main defect of the existing procedure, its overprediction of palaeo-temperatures before the start of flat subduction. Flat subduction may thus also explain the growing body of evidence, from metamorphic and structural studies (e.g., Okay, 2001; Rimmelé et al., 2003; Erdoğan and Güngör, 2004; cf. Ring et al., 2001; Gessner et al., 2004), for reverse-faulting and prograde metamorphism within the Menderes Massif at this time. It may also account for the observed folding of the early (i.e., Early Miocene) part of the sedimentary sequences in the Selendi Basin and its neighbours in the northern Menderes Massif (e.g., Westaway et al., 2004; Purvis and Robertson, 2004), these localities probably being near the northern limit of the flat subduction, and the SW–NE trend of these basins may thus reflect folding oriented along older thrust structures associated with closure of the İzmir-Ankara-Erzincan ocean (Fig. 2).

Second, the cooling effect will cause the ~300 or ~350 °C thermal boundary at the base of the brittle upper crust to deepen, which will increase the local pressure acting on the lower crust in this region, which will act to make lower crust flow out from beneath this region to beneath its surroundings (e.g., Westaway, 2002b). Localised subsidence can thus be expected to result from this component of crustal thinning, which (maybe in combination with the active reverse-faulting also occurring, as noted above) can be expected to have created localised depocentres for accumulation of sedimentary sequences, such as the marine "Denizli Molasse" and the more widespread early (pre-extensional) terrestrial parts of the sedimentary sequences in what are now the hanging-walls of the AFZ and BMFZ. The widespread observation in western Turkey (cf. Westaway et al., 2005) of Late Cenozoic terrestrial sediment that is unrelated to crustal extension can thus tentatively be explained. Furthermore, the presence of Late Oligocene–Early Miocene marine sediment indicates that the land surface in this region was locally below sea-level at this time, despite the crustal shortening inferred to have been occurring, which is explicable if the inferred thickening of the brittle upper crust (Fig. 6(b)) was exceeded by the outflow of lower crust due to the contemporaneous cooling (cf. Westaway, 2002a,b). Many studies (e.g., Bozkurt, 2000) have inferred that in the Late Oligocene/Early Miocene western Turkey formed a high plateau, possibly analogous to Tibet; the presence of marine sediments from this time indicates on the contrary that at least part of this region was at sea-level. Several recent studies (e.g., Westaway et al., 2003a, 2004, 2005; Demir et al., 2004) have indeed shown quantitatively that much of western Turkey's present relief has developed during the Late Cenozoic; on this time scale this region has thus experienced surface uplift, not subsidence. The present interpretation suggests that this phase of regional uplift was preceded by subsidence caused by cooling due to flat subduction. However, calculating the magnitude of this subsidence effect, and assessing any correction that may need to be applied to the calculations of subsequent uplift, are beyond the scope of this study.

Fig. 6(c) shows the regional deformation sense inferred to have been occurring in the (?) Middle Miocene, after flat subduction ended. A new phase of steep subduction of oceanic lithosphere of the Eastern Mediterranean Basin is shown beginning at the Hellenic Trench, where it continues to the present day. The former flat slab is assumed to have since become assimilated into the surrounding asthenosphere. The base of the brittle upper crust is shown advecting upwards as the geotherm begins to adjust back to its normal value for a single layer of lithosphere, which would be expected to accompany inflow of lower crust, balancing the earlier outflow. The associated heating of the mantle lithosphere could be expected to result in release of relatively volatile material, potentially explaining the widespread Middle Miocene volcanism of western Turkey (e.g., Seyitoğlu, 1997; Yılmaz et al., 2000; Westaway et al., 2004, 2005). Finally, in Fig. 6(d) crustal extension is shown beginning at ~7 Ma. As previously discussed (e.g., Westaway, 2003; Westaway et al., 2005) this timing relates to several regional factors, including the start of slip on the North Anatolian Fault Zone and the increased slab pull force at the Hellenic Trench (cf. Meijer and Wortel, 1997) but may also have been facilitated by the progressive weakening of the lithosphere presumed to have accompanied its continued heating after the ending of flat subduction.

It is evident that the timing of any flat subduction is quite tightly constrained. It can have lasted for no more than ~20–25 million years in the south, and progressively less farther north. As previous calculations have indicated, for such a brief phase of subduction to have caused temperature perturbations of the observed magnitude requires both relatively thin (~60–75 km) lithosphere and relatively high erosion rates, no less than ~0.4–0.5 mm a^{-1}. However, as already noted, these estimates may exceed the true erosion rates because effects of radiogenic heating have not been considered when calculating these cooling histories. Nonetheless, these rates are substantially higher than the ~0.1 mm a^{-1} typical erosion rate estimates for the Middle–Late Pleistocene and Holocene obtained for western Turkey by Westaway (1994b) and Westaway et al. (2004). However, the calculations of Westaway (1994b) were for net erosion from the whole region; for instance, they do not include material eroded from the central Menderes Massif and deposited in neighbouring grabens by alluvial fans. It can anyway be presumed that erosion rates experienced an overall decrease as metamorphic basement became progressively exhumed, and the overlying deposits (presumed less well lithified) were removed. Such effects are not included in the geothermal calculations in this study, although they have been investigated elsewhere (e.g., Westaway, 2002a,b). A direct confirmation of the erosion rates (and any variations) proposed for the mid-Cenozoic by analysing the regional mass balance, including both terrestrial and offshore sedimentation, would be extremely difficult, and is beyond the scope of this study.

No attempt has been made to constrain any cooling and exhumation calculations in this study using (?) Oligocene palaeo-temperatures and -pressures derived from metamorphic mineral assemblages, such as the ~530 °C and ~8 kbar (~30 km depth) estimate for the southern part of the central Menderes Massif north of Aydın (Okay, 2001), or the ~430–550 °C and ~6-8 kbar (~22–30 km) estimate for the Çine Massif between Yatağan and Bafa Lake (Whitney and Bozkurt, 2002), or the ~430 °C and ~9 kbar (~33 km depth) estimate for the western Çine Massif at Kurudere (Rimmelé et al., 2003) (Fig. 2). This is because such results show significant inconsistencies between independent studies of the same localities (cf. Rimmelé et al., 2003) and have also typically not been co-located with the thermochronologic studies. However, because these data have not been used to constrain the predicted cooling history solutions, comparison with them can be used as a test of the predictions, as well as providing a possible indication of which of the available data on peak metamorphic conditions are valid in cases where they conflict.

For the schists at the southern margin of the Çine Massif, the estimated temperature range of ~430–550 °C at the start of exhumation from the peak metamorphic conditions (Whitney and Bozkurt, 2002) is entirely consistent with the subsequent temperature history deduced from the thermochronology and fitted using the present thermal modelling (Fig. 3(e)), but the maximum depth of burial predicted for this region is 18.2 km (for exhumation at 0.52 mm a^{-1} since 35 Ma; Fig. 3(e)), suggesting an initial pressure of ~5 kbar. However, the ~6–8 kbar pressure range estimated by Whitney and Bozkurt (2002) did not represent an error margin, but a systematic error between techniques: geobarometry indicated ~8 kbar but structural data and mineral assemblages indicated <~6 kbar. The latter data may well be consistent with the present thermal modelling; the former would require faster erosion and a thicker lithosphere than has so far been assumed. Regarding the gneiss in the interior of this massif, Gessner et al. (2004) inferred that the peak metamorphic conditions were attained in the Late Precambrian during the Pan-African orogeny, and thus have no bearing on the Cenozoic thermal history. This is also consistent with the present modelling, which indicates that the thermochronologic data (many of which came from sites within this gneiss; Fig. 2) fit thermal histories that are consistent with the conditions deduced within the adjacent schists during the Early Cenozoic (e.g., Whitney and Bozkurt, 2002); these schists can thus be presumed to provide good indications of the contemporaneous conditions in the adjacent gneisses.

For the AFZ footwall, Ring et al. (1999) briefly mentioned that the peak temperature may have exceeded 600 °C in the area northeast of Ödemiş (Fig. 2), but no details were provided. Subsequent studies (e.g., Candan et al., 2001; Ring et al., 2001) have indicated that this region's peak metamorphic conditions were reached during the Late Precambrian ('Pan-African') crustal consolidation, making it relatively difficult to infer conditions at later stages of polyphase metamorphism. Such studies have also been somewhat noncommittal as to whether the most recent phase of metamorphism identified locally occurred in the Cenozoic. Assuming that it did, Candan et al. (2001) reported a temperature of 623 °C and a pressure of 7 kbar (depth ~26 km) in the area roughly halfway between Alaşehir and Kiraz (Fig. 2); Ring et al. (2001) reported a temperature of 620 °C and a pressure of 6.4–6.5 kbar (depth ~24 km) in the area between Kiraz and Ödemiş (Fig. 2). The solutions in Fig. 3(f) indicate slightly higher initial temperatures, but — as elsewhere in the region — the thermochronologic data to which they have been fitted were not from the same places as the sites that indicate the earlier metamorphic conditions. Improved thermal modelling must await the availability of more systematic metamorphic and thermochronologic datasets, preferably co-located with each other.

The results of this study help to reconcile geodetic and geological estimates for extension rates across western Turkey. Seismic moment summation indicates rates of several millimetres per year, at least (e.g., Westaway, 1994b). GPS geodesy indicates that, relative to Eurasia, the SW velocity increases southwestward across western Turkey by ~10 mm a^{-1}, from ~20 to ~30 mm a^{-1} (e.g., McClusky et al., 2000), with the extension rate across the AFZ estimated as $\sim 6 \pm 2$ mm a^{-1} (Westaway et al., 2004) . If extension at comparable rates has been occurring since ~7 Ma (cf. Westaway, 2003, 2004a), then ~70 km of extension is required, with at least ~30 km on the AFZ. The structural interpretation by Cohen et al. (1995, Fig. 11(a)) indicates that the presently active relatively steep normal faults within the AFZ have taken up 7 km of extension (estimated from their combined heave), roughly as expected from the geodetically observed extension rate if these faults have been active since the late Early Pleistocene (cf. Westaway, 1998; see also earlier discussion). Hetzel et al. (1995b, Fig. 14) indicate that the formerly active presently low-angle normal fault that was superseded then took up at least 11 km of

extension; probably significantly more, as its hanging-wall cutoff is not exposed and its original footwall cutoff has evidently been eroded. Assuming that this fault formed with a uniform dip of δ_o from the Earth's surface to a depth of D_o, and had a dip δ and a vertical extent D when slip on it ceased, then its heave E can be estimated as

$$E = D\cot(\delta) - D_o\cot(\delta_o), \quad (37)$$

assuming extension accommodated by distributed vertical simple shear (Westaway and Kusznir, 1993). Taking δ_o at the initiation of the AFZ as 64° (see earlier discussion), D_o as ~20 km, D as ~15 km, and δ when it ceased to be active as somewhere between ~30° (cf. Jackson and McKenzie, 1983) and its present-day ~16° dip, then E can be estimated as between ~16 and ~42 km, probably closer to the former value for δ 30°. This indicates a time-averaged extension rate on this fault approaching ~3 mm a^{-1} if it was active for 6 million years (from ~7 to ~1 Ma), or more if δ was lower when this slip ceased or if slip on it ceased earlier. There is thus agreement to within a factor of two between these independent geodetic, seismological, and structural estimates of extension rates, suggesting that this region's extension history is now reasonably well-quantified. The results of this investigation also illustrate the general point that evolution of the continental lithosphere typically occurs under non-steady-state thermal regimes (cf. Westaway, 2004c).

The principal difficulty with the present conclusions concerns reconciling the inference of flat subduction of the African plate during the mid-Tertiary with the results of earlier tomographic investigations of the geometry of this subducting slab. Early investigations of this region noted the ~150–200 km depth limit of seismicity within the modern Hellenic Benioff zone, from which a young age for the start of this subduction was inferred, such as the ~5 Ma estimate by McKenzie (1978). Le Pichon and Angelier (1979) likewise estimated the age of this subduction as ~13 Ma, a similar value to that inferred in the present study even though the underlying reasoning is entirely different. However, more recent studies (e.g., Meulenkamp et al., 1988; Laigle et al., 2004) have proposed that this depth limit of seismicity relates to a stability threshold for aseismic slip, and so does not mark the full downdip extent of this subducting slab. Subsequent studies of seismic travel-time tomography (e.g., Meulenkamp et al., 1988; Spakman et al., 1988) inferred (from relatively high seismic wave velocities, indicating material that is cooler than its surroundings) that this slab persists to a depth of at least 600 km and is at least 800 km long, suggesting that its subduction began as early as ~40 Ma. If this view is correct, there can be no basis for subduction of a separate flat slab, also derived from the African plate, between ~40 and ~15 Ma, as suggested in the present study.

However, a more recent tomographic study by Spakman et al. (1993) reported that this Hellenic slab reaches a depth of ~800–900 km, with a total downdip length of ~1400–1500 km (see their Fig. 10). This raises a major difficulty, because the total convergence between the African and Eurasian plates in the vicinity of the Aegean Sea since their present phase of relative motion began in the Palaeocene (~56 Ma) is estimated as only ~900 km (e.g., Garfunkel, 2004). Even after allowing, say, an additional ~200 km of slab length to accommodate Aegean extension and slip on the NAFZ, this tomographic slab image is much longer than seems feasible from other geological information.

It is evident that such tomographic investigations can reliably resolve shallow thermal structure, related to lateral variations in thickness and thermal age of the lithosphere (e.g., Goes et al., 1999; Goes and van der Lee, 2002; van der Lee, 2002); they have indeed been extensively used for this purpose in my own rheological modelling studies (e.g., Westaway et al., 2003b; Westaway, 2004b). However, at an early stage in the development of this tomographic technique, the question was raised whether it has the effect of smearing out a localised seismic velocity anomaly for a short subducting slab into a spatially much larger anomaly of smaller magnitude, because some seismic raypaths traverse the slab in the downdip direction. After conducting appropriate sensitivity tests, Spakman and Nolet (1988) asserted that this is not so for the Hellenic slab. However, a test of this view is possible, using the tomographic image of the subducting slab beneath the Tyrrhenian Sea in the central Mediterranean. This subduction system is revealed by a zone of seismicity that plunges WNW at ~65° to ~500 km depth (e.g., Pasquale et al., 1999); the total length of this slab that is seismic can thus be roughly estimated as ~500 km/cos (65°) or ~550 km. Since ~8 Ma (e.g., Argnani and Savelli, 1999; Faccenna et al., 2001), this subduction has accommodated eastsoutheastward motion of Calabria, southern mainland Italy, relative to Sardinia, against which Calabria was previously juxtaposed; involving motion that has been much faster than, and roughly perpendicular to, the northward convergence between the African and Eurasian plates. One thus expects the length of this slab to roughly equal the present-day distance between Sardinia and Calabria, which is indeed ~550 km, leaving no scope for this slab to be longer. However, its

tomographic image (see Spakman et al., 1993, Fig. 10) shows a concentrated seismic velocity anomaly down to ~350–400 km, then a more diffuse anomaly persisting downward and WNW for another ~600 km, making it perhaps ~400 km longer than the true extent of this slab.

The Hellenic slab has a strong velocity anomaly plunging at ~25° down to ~200 km depth (see Spakman et al., 1993, Fig. 3), and roughly coinciding with its seismicity, so this part of this slab can be estimated as ~350 km long. Allowing, as before, ~200 km of it to accommodate Aegean extension and NAFZ slip, one is left with ~150 km taken up by Africa-Eurasia convergence, which implies an age of subduction of ~15 Ma at a realistic present-day convergence rate of ~10 mm a^{-1} (cf. McClusky et al., 2000). The earliest studies of this region may well thus have been correct to suggest the simple view that this dipping zone of seismicity marks the full downdip extent of this slab. One can indeed estimate that, of the ~900 km of Africa-Eurasia convergence predicted in this region since the Palaeocene (Garfunkel, 2004), ~250 km of it was accommodated by closure of the Neotethyan ocean basins before ~40 Ma and ~500 km of it occurred by flat subduction during an estimated age span from ~40 to ~15 Ma, with the remaining ~150 km taken up by the modern subduction system.

A related question concerns whether tomography can reveal any evidence for the present location of the slab that is inferred to have subducted beneath western Turkey at a low angle. Tomography does reveal a zone of relatively high seismic velocity, starting at ~300 km depth beneath the area of Çanakkale (Fig. 1) and persisting northeastward, plunging gently, for ~500 km (see, e.g., Meulenkamp et al., 1988, Fig. 3; Spakman et al., 1988, Fig. 2, or Spakman et al., 1993, Figs. 9 and 10). However, although this feature seems clear enough when the seismic velocity anomaly pattern is measured relative to the Jeffreys–Bullen standard, it virtually disappears (see Figs. 9 and 10 of Spakman et al., 1993) when measured relative to an alternative velocity model, derived from Paulssen (1987). It thus seems appropriate to postpone further discussion of these controversial tomographic images until it can be established which of their features are 'real' and which may be artefacts of the technique or of choice of reference model.

6. Conclusions

It is proposed that the geothermal regime within the Menderes Massif in western Turkey was affected during the mid-Cenozoic by flat northward subduction of oceanic lithosphere of the Eastern Mediterranean Basin. This process can be readily incorporated into an evolutionary model for this region (Fig. 6), and can account for many observations from within this massif, including dramatic cooling of the crust (Fig. 3) that has been previously been considered a consequence of low-angle normal faulting. Since no convincing independent evidence of this process exists within this massif, it is inferred that it has not been affected by low-angle normal faulting during the mid- to Late Cenozoic. The available thermochronologic evidence indicates that extension began on one of the principal active normal fault zones in western Turkey, the Alaşehir Fault Zone, at ~7 Ma, consistent with the Late Miocene onset of this region's extension-related volcanism (cf. Westaway et al., 2005).

Acknowledgements

I thank Klaus Gessner and Aral Okay for thoughtful and constructive reviews. This study contributes to International Geoscience Programme 518: 'Fluvial sequences as evidence for landscape and climatic evolution in the Late Cenozoic.'

References

Akgün, F., Sözbilir, H., 2001. A palynostratigraphic approach to the SW Anatolian molasse basin: Kale-Tavas Molasse and Denizli Molasse. Geodinamica Acta 14, 71–93.

Aldanmaz, E., Pearce, J.A., Thirlwall, M.F., Mitchell, J.G., 2000. Petrogenetic evolution of Late Cenozoic, post-collision volcanism in western Anatolia Turkey. Journal of Volcanology and Geothermal Research 102, 67–95.

Argnani, A., Savelli, C., 1999. Cenozoic volcanism and tectonics in the southern Tyrrhenian Sea: space–time distribution and geodynamic significance. Journal of Geodynamics 27, 409–432.

Becker-Platen, J.D., Benda, L., Steffens, P., 1977. Litho-und biostratigraphische Deutung radiometrischer Altersbestimmungen aus der Jungtertiär der Türkei. Geologisches Jahrbuch, Series B 25, 139–167.

Besang, C., Eckhardt, F.J., Harre, W., Kreuzer, H., Müller, P., 1977. Radiometrische Altersbestimmungen an Neogenen Eruptivgesteinen der Türkei. Geologisches Jahrbuch, Series B 25, 3–36.

Bozkurt, E., 2000. Timing of extension on the Büyük Menderes Graben, western Turkey, and its tectonic implications. In: Bozkurt, E., Winchester, J.A., Piper, J.D.A. (Eds.), Tectonics and Magmatism of Turkey and the Surrounding Area, vol. 173. Geological Society of London Spececial Publication, pp. 385–403.

Bozkurt, E., 2001a. Neotectonics of Turkey—a synthesis. Geodinamica Acta 14, 3–30.

Bozkurt, E., 2001b. Late Alpine evolution of the central Menderes Massif, western Turkey. International Journal of Earth Sciences 89, 728–744.

Bozkurt, E., 2002. Discussion on "Extensional folding in the Alaşehir (Gediz) Graben, western Turkey" by Seyitoğlu, G., Çemen, İ,

Tekeli, O. Journal of the Geolological Society of London 159, 105–109.
Bozkurt, E., 2003. Origin of NE-trending basins in western Turkey. Geodinamica Acta 16, 61–81.
Bozkurt, E., 2004. Granitoid rocks of the southern Menderes Massif (southwestern Turkey): field evidence for Tertiary magmatism in an extensional shear zone. International Journal of Earth Sciences 93, 52–71.
Bozkurt, E., Park, R.G., 1994. Southern Menderes Massif: an incipient metamorphic core complex in western Anatolia, Turkey. Journal of the Geolological Society of London 151, 213–216.
Bozkurt, E., Sözbilir, H., 2004. Tectonic evolution of the Gediz Graben: field evidence for an episodic, two-stage extension in western Turkey. Geological Magazine 141, 63–79.
Candan, O., Dora, O., Oberhänsli, R., Çetinkaplan, M., Partzsch, J., Warkus, F., Dürr, S., 2001. Pan-African high-pressure metamorphism in the Precambrian basement of the Menderes Massif, western Anatolia, Turkey. International Journal of Earth Sciences 89, 793–811.
Carslaw, H.S., Jaeger, J.C., 1959. Conduction of Heat in Solids, 2nd ed. Clarendon Press, Oxford. 510 pp.
Cohen, H.A., Dart, C.J., Akyüz, H.S., Barka, A.A., 1995. Syn-rift sedimentation and structural development of the Gediz and Büyük Menderes grabens, western Turkey. Journal of the Geolological Society of London 152, 629–638.
Collins, A.S., Robertson, A.H.F., 1998. Processes of Late Cretaceous to Late Miocene episodic thrust-sheet translation in the Lycian Taurides, SW Turkey. Journal of the Geolological Society of London 155, 759–772.
Demir, T., Yeşilnacar, İ., Westaway, R., 2004. River terrace sequences in Turkey: sources of evidence for lateral variations in regional uplift. Proceedings of the Geologists' Association, vol. 115, pp. 289–311.
Dumitru, T.A., Gans, P.B., Foster, D.A., Miller, E.L., 1991. Refrigeration of the western Cordilleran lithosphere during Laramide shallow-angle subduction. Geology 19, 1145–1148.
Ercan, T., Dincel, A., Metin, S., Türkecan, A., Günay, E., 1978. Geology of the Neogene basins in Uşak region. Bulletin of the Geological Society of Turkey 21, 97–106 (in Turkish with English summary).
Erdoğan, T., Güngör, T., 2004. The problem of the core-cover boundary of the Menderes Massif and an emplacement mechanism for regionally extensive gneissic granites, western Anatolia (Turkey). Turkish Journal of Earth Science 13, 15–36.
England, P.C., Thompson, A., 1986. Some thermal and tectonic models for crustal melting in continental collision zones. In: Coward, M.P., Ries, A.C. (Eds.), Collision Tectonics, Geological Society of London Special Publication, vol. 19, pp. 83–94.
Faccenna, C., Becker, T.W., Lucente, F.P., Jolivet, L., Rossetti, F., 2001. History of subduction and back-arc extension in the Central Mediterranean. Geophysical Journal International 145, 809–820.
Garfunkel, Z., 2004. Origin of the Eastern Mediterranean basin: a reevaluation. Tectonophysics 391, 11–34.
Gessner, K., Piazolo, S., Güngör, T., Ring, U., Kröner, A., Passchier, C.W., 2001a. Tectonic significance of deformation patterns in granitoid rocks of the Menderes nappes, Anatolide belt, SW Turkey. International Journal of Earth Sciences 89, 766–780.
Gessner, K., Ring, U., Johnson, C., 2001b. An active bivergent rolling-hinge detachment system: Central Menderes metamorphic core complex in western Turkey. Geology 29, 611–614.
Gessner, K., Ring, U., Passchier, C.W., Güngör, T., 2001c. How to resist subduction: evidence for large-scale out-of-sequence thrusting during Eocene collision in western Turkey. Journal of the Geological Society of London 158, 769–784.
Gessner, K., Collins, A.S., Ring, U., Güngör, T., 2004. Structural and thermal history of poly-orogenic basement: U–Pb geochronology of granitoid rocks in the southern Menderes Massif, western Turkey. Journal of the Geological Society of London 161, 93–101.
Goes, S., Spakman, W., Bijwaard, H., 1999. A lower mantle source for Central European volcanism. Science 286, 928–931.
Goes, S., van der Lee, S., 2002. Thermal structure of the North American uppermost mantle inferred from seismic tomography. Journal of Geophysical Research 107 (B3). doi:10.1029/2000JB000049 (published online).
Gökçen, N., 1979. Stratigraphy and palaeogeography of the Neogene sequences of the Denizli-Muğla region (SW Anatolia). Annales Géologiques des Pays Helleniques, 467–474 (volume out of series).
Gökçen, N., 1982. The otracod biostratigraphy of the Denizli-Muğla Neogene sequence. Yerbilimleri 9, 111–131 (in Turkish with English abstract).
Gutscher, M.-A., Spakman, W., Bijwaard, H., Engdahl, E.R., 2000. Geodynamics of flat subduction: seismicity and tomographic constraints from the Andean margin. Tectonics 19, 814–833.
Hakyemez, H.Y., 1989. Kale-Kurbalik (GB Denizli) bölgesindeki Senozoyik yaşlı çökel kayaların jeolojisi ve stratigrafisi. MTA Dergisi 109, 9–21.
Hetzel, R., Reischmann, T., 1996. Intrusion age of Pan-African augen gneiss in the southern Menderes Massif and the age of cooling after Late Cretaceous—Tertiary ductile extensional deformation. Geological Magazine 133, 565–572.
Hetzel, R., Passchier, C.W., Ring, U., Dora, Ö.O., 1995a. Bivergent extension in orogenic belts: the Menderes Massif (southwestern Turkey). Geology 23, 455–458.
Hetzel, R., Ring, U., Akal, C., Troesch, M., 1995b. Miocene NNE-directed extensional unroofing in the Menderes Massif, southwestern Turkey. Journal of the Geological Society of London 152, 639–654.
Hetzel, R., Passchier, C.W., Ring, U., Dora, Ö.O., 1996. Reply to comment by R. Westaway on "Bivergent extension in orogenic belts: the Menderes massif (southwestern Turkey)" by R. Hetzel, C.W. Passchier, U. Ring, and Ö.O. Dora. Geology 24, 94–95.
Ilkışık, O.M., 1995. Regional heat flow in western Anatolia using silica temperature estimates from thermal springs. Tectonophysics 244, 175–184.
Işik, V., Tekeli, O., 2001. Late orogenic crustal extension in the northern Menderes Massif (western Turkey): evidence for metamorphic core complex formation. International Journal of Earth Sciences 89, 757–765.
Jackson, J.A., 1987. Active normal faulting and crustal extension. In: Coward, M.P., Dewey, J.F., Hancock, P.L. (Eds.), Continental Extensional Tectonics, Geological Society of London Special Publication, vol. 28, pp. 3–17.
Jackson, J.A., McKenzie, D.P., 1983. The geometrical evolution of normal fault systems. Journal of Structural Geology 5, 471–482.
Jackson, J.A., McKenzie, D.P., 1988. Rates of active deformation in the Aegean Sea and surrounding regions. Basin Research 1, 121–128.
Jackson, J.A., White, N.J., 1989. Normal faulting in the upper continental crust; observations from regions of active extension. Journal of Structural Geology 11, 15–36.
Koçyiğit, A., Yusufoğlu, H., Bozkurt, E., 1999. Evidence from the Gediz graben for episodic two-stage extension in western Turkey. Journal of the Geolological Society of London 156, 605–616.

Koralay, O.E., Satır, M., Dora, O.Ö., 2001. Geochemical and geochronological evidence for Early Triassic calc-alkaline magmatism in the Menderes Massif, western Turkey. International Journal of Earth Sciences 89, 822–835.

Lachenbruch, A.H., 1970. Crustal temperature and heat production: implications of the linear heat flow relation. Journal of Geophysical Research 75, 3291–3300.

Laigle, M., Sachpazi, M., Hirn, A., 2004. Variation of seismic coupling with slab detachment and upper plate structure along the western Hellenic subduction zone. Tectonophysics 391, 85–95.

Le Pichon, X., Angelier, J., 1979. The Hellenic arc and trench system: a key to the evolution of the Eastern Mediterranean area. Tectonophysics 60, 1–42.

Lips, A.L.W., Cassard, D., Sözbilir, H., Yılmaz, H., Wijbrans, J.R., 2001. Multistage exhumation of the Menderes Massif, western Anatolia (Turkey). International Journal of Earth Sciences 89, 781–792.

McClusky, S., et al., 2000. Global Positioning System constraints on plate kinematics and dynamics in the eastern Mediterranean and Caucasus. Journal of Geophysical Research 105, 5695–5719.

McDougall, I., Harrison, T.M., 1999. Geochronology and Thermochronology by the $^{40}Ar/^{39}Ar$ Method, 2nd edition. Oxford University Press. 269 pp.

McKenzie, D.P., 1978. Some remarks on the development of sedimentary basins. Earth and Planetary Science Letters 40, 25–32.

Meijer, P.T., Wortel, M.J.R., 1997. Present-day dynamics of the Aegean region: a model analysis of the horizontal pattern of stress and deformation. Tectonics 16, 879–895.

Meulenkamp, J.E., Wortel, M.J.R., van Wamel, W.A., Spakman, W., Hoogerduyn Strating, E., 1988. On the Hellenic subduction zone and the geodynamic evolution of Crete since the late middle Miocene. Tectonophysics 146, 203–215.

Okay, A., 2001. Stratigraphic and metamorphic inversions in the central Menderes Massif: a new structural model. International Journal of Earth Sciences 89, 709–727.

Okay, A., Satır, M., 2000. Coeval plutonism and metamorphism in a latest Oligocene metamorphic core complex in northwest Turkey. Geological Magazine 137, 495–516.

Özer, S., Sözbilir, H., 2003. Presence and tectonic significance of Cretaceous rudist species in the so-called Permo-Carboniferous Goktepe Formation, central Menderes metamorphic massif, western Turkey. International Journal of Earth Sciences 92, 397–404.

Pasquale, V., Verdoya, M., Chiozzi, P., 1999. Thermal state and deep earthquakes in the southern Tyrrhenian. Tectonophysics 306, 435–448.

Paulssen, H., 1987. Lateral inhomogeneity of Europe's upper mantle as inferred from modeling of broad-band body waves. Geophysical Journal of the Royal Astronomical Society 91, 171–199.

Proffett Jr., J.M., 1977. Cenozoic geology of the Yerington District, Nevada, and implications for the nature and origin of Basin and Range faulting. Geological Society of America Bulletin 88, 247–266.

Purvis, M., Robertson, A.H.F., 2004. A pulsed extension model for the Neogene—recent E–W trending Alaşehir Graben and the NE–SW trending Selendi and Gördes Basins, western Turkey. Tectonophysics 391, 171–201.

Rimmelé, G., Oberhänsli, R., Goffé, B., Jolivet, L., Candan, O., Çetinkaplan, M., 2003. First evidence of high-pressure metamorphism in the "Cover Series" of the southern Menderes Massif. Tectonic and metamorphic implications for the evolution of SW Turkey. Lithos 71, 19–46.

Ring, U., Gessner, K., Güngör, T., Passchier, C.W., 1999. The Menderes Massif of western Turkey and the Cycladic Massif in the Aegean; do they really correlate? Journal of the Geological Society of London 156, 3–6.

Ring, U., Willner, A.P., Lackmann, W., 2001. Stacking of nappes with different pressure–temperature paths; an example from the Menderes Nappes of western Turkey. American Journal of Science 301, 912–944.

Ring, U., Johnson, C., Hetzel, R., Gessner, K., 2003. Tectonic denudation of a Late Cretaceous—Tertiary collisional belt: regionally-symmetric cooling patterns and their relation to extensional faults in the Anatolide Belt of western Turkey. Geological Magazine 140, 421–441.

Sarıca, N., 2000. The Plio-Pleistocene age of Büyük Menderes and Gediz grabens and their tectonic significance on N–S extensional tectonics in west Anatolia: mammalian evidence from the continental deposits. Geological Journal 25, 1–24.

Saunders, P., Priestley, K., Taymaz, T., 1998. Variations in the crustal structure beneath western Turkey. Geophysical Journal International 134, 373–389.

Seyitoğlu, G., 1997. Late Cenozoic tectono-sedimentary development of the Selendi and Uşak-Güre basins: a contribution to the discussion on the development of east–west and north trending basins in western Turkey. Geological Magazine 134, 163–175.

Seyitoğlu, G., Scott, B., 1996. Age of the Alaşehir graben (west Turkey) and its tectonic implications. Geological Journal 31, 1–11.

Seyitoğlu, G., Tekeli, O., úemen, I., Sen, S, Isik, V., 2002. The role of the flexural rotation/rolling hinge model in the tectonic evolution of the Alasehir Graben, western Turkey. Geological Magazine 139, 15–26Spakman, W., Nolet, G., 1988. Imaging algorithms, accuracy and resolution in delay time tomography. In: Vlaar, N.J., Nolet, G., Wortel, M.J.R., Cloetingh, S.A.P.L. (Eds.), Mathematical Geophysics: A Survey of Recent Developments in Seismology and Geophysics. Reidel, Dordrecht, pp. 155–188.

Spakman, W., Wortel, M.J.R., Vlaar, N.J., 1988. The Hellenic subduction zone; a tomographic image and its geodynamic implications. Geophysical Research Letters 15, 60–63.

Spakman, W., van der Lee, S., van der Hilst, R., 1993. Travel-time tomography of the European–Mediterranean mantle down to 1400 km. Physics of the Earth and Planetary Interiors 79, 3–74.

Stüwe, K., White, L., Brown, R., 1994. The influence of eroding topography on steady-state isotherms. Application to fission track analysis. Earth and Planetary Science Letters 124, 63–74.

Thompson, A.B., England, P.C., 1984a. Pressure–temperature–time paths of regional metamorphism: I. Heat transfer during the evolution of regions of thickened continental crust. Journal of Petrology 25, 894–928.

Thompson, A.B., England, P.C., 1984b. Pressure–temperature–time paths of regional metamorphism: II. Their inference and interpretation using mineral assemblages in metamorphic rocks. Journal of Petrology 25, 929–955.

Ünay, E., de Bruijn, H., 1998. Plio-Pleistocene rodents and lagomorphs from Anatolia. Mededelingen Nederlands Instituut voor Toegepaste Geowetenschappen TNO, vol. 60, pp. 431–466.

Ünay, E., Göktaş, F., Hakyemez, H.Y., Avşar, M., Şan, Ö., 1995. Dating of the sediments exposed at the northern part of the Büyük Menderes Graben on the basis of Arvicolidae (Rodentia Mammalia). Geological Bulletin of Turkey 38, 75–80.

van der Lee, S., 2002. High-resolution estimates of lithospheric thickness from Missouri to Massachusetts, USA. Earth and Planetary Science Letters 203, 15–23.

Verge, N.J., 1993. The exhumation of the Menderes Massif metamorphic complex of western Anatolia. Seventh meeting of the European Union of Geosciences; abstract supplement. Terra Abstracts 5, 249 (abstract).

Westaway, R., 1990. Block rotation in western Turkey: 1. Observational evidence. Journal of Geophysical Research 95, 19857–19884.

Westaway, R., 1994a. Reevaluation of extension in the Pearl River Mouth basin, South China Sea: implications for continental lithosphere deformation mechanisms. Journal of Structural Geology 16, 823–838.

Westaway, R., 1994b. Evidence for dynamic coupling of surface processes with isostatic compensation in the lower crust during active extension of western Turkey. Journal of Geophysical Research 99, 20203–20223.

Westaway, R., 1996. Comment on "Bivergent extension in orogenic belts: the Menderes massif (southwestern Turkey)" by R. Hetzel, C.W. Passchier, U. Ring, and Ö.O. Dora. Geology 24, 93–94.

Westaway, R., 1998. Dependence of active normal fault dips on lower-crustal flow regimes. Journal of the Geological Society of London 155, 233–253.

Westaway, R., 1999. The mechanical feasibility of low-angle normal faulting. Tectonophysics 308, 407–443 (Correction: Tectonophysics, 341, 237–238).

Westaway, R., 2001. Flow in the lower continental crust as a mechanism for the Quaternary uplift of the Rhenish Massif, north-west Europe. In: Maddy, D., Macklin, M., Woodward, J. (Eds.), River Basin Sediment Systems: Archives of Environmental Change. Balkema, Abingdon, England, pp. 87–167.

Westaway, R., 2002a. The Quaternary evolution of the Gulf of Corinth, central Greece: coupling between surface processes and flow in the lower continental crust. Tectonophysics 348, 269–318.

Westaway, R., 2002b. Geomorphological consequences of weak lower continental crust, and its significance for studies of uplift, landscape evolution, and the interpretation of river terrace sequences. Netherlands Journal of Geosciences 81, 283–304.

Westaway, R., 2002c. Long-term river terrace sequences: evidence for global increases in surface uplift rates in the Late Pliocene and early Middle Pleistocene caused by flow in the lower continental crust induced by surface processes. Netherlands Journal of Geosciences 81, 305–328.

Westaway, R., 2003. Kinematics of the Middle East and Eastern Mediterranean updated. Turkish Journal of Earth Sciences 12, 5–46.

Westaway, R., 2004a. Kinematic consistency between the Dead Sea Fault Zone and the Neogene and Quaternary left-lateral faulting in SE Turkey. Tectonophysics 391, 203–237.

Westaway, R., 2004b. Pliocene and Quaternary surface uplift revealed by sediments of the Loire-Allier river system, France. Quaternaire 15, 103–115.

Westaway, R., 2004c. Review of "The steady-state orogen: concepts, field observations, and models", edited by Frank Pazzaglia and Peter Knuepfer (special volume 151 of American Journal of Science, Yale University Press, Connecticut, USA, 2001). Quaternary Science Reviews 23, 215–218.

Westaway, R., Kusznir, N.J., 1993. Fault and bed 'rotation' during continental extension: block rotation or vertical shear? Journal of Structural Geology 15, 753–770 (Correction: Journal of Structural Geology, 151391).

Westaway, R., Pringle, M., Yurtmen, S., Demir, T., Bridgland, D., Rowbotham, G., Maddy, D., 2003a. Pliocene and Quaternary surface uplift of western Turkey revealed by long-term river terrace sequences. Current Science 84, 1090–1101.

Westaway, R., Bridgland, D., Mishra, S., 2003b. Rheological differences between Archaean and younger crust can determine rates of Quaternary vertical motions revealed by fluvial geomorphology. Terra Nova 15, 287–298.

Westaway, R., Pringle, M., Yurtmen, S., Demir, T., Bridgland, D., Rowbotham, G., Maddy, D., 2004. Pliocene and Quaternary regional uplift in western Turkey: the Gediz river terrace staircase and the volcanism at Kula. Tectonophysics 391, 121–169.

Westaway, R., Guillou, H., Yurtmen, S., Demir, T., Rowbotham, G., 2005. Investigation of the conditions at the start of the present phase of crustal extension in western Turkey, from observations in and around the Denizli region. Geodinamica Acta 18, 313–343.

Whitney, D.L., Bozkurt, E., 2002. Metamorphic history of the southern Menderes Massif, western Turkey. Geological Society of America Bulletin 114, 829–838.

Whitney, D.L., Hamilton, M.A., 2004. Timing of high-grade metamorphism in central Turkey and the assembly of Anatolia. Journal of the Geological Society of London 161, 823–828.

Yılmaz, Y., Genç, S.C., Gürer, F., Bozcu, M., Yılmaz, K., Karacık, Z., Altunkaynak, Ş, Elmas, A., 2000. When did the Aegean grabens begin to develop? In: Bozkurt, E., Winchester, J.A., Piper, J.D.A. (Eds.), Tectonics and Magmatism in Turkey and the Surrounding Area, Geological Society of London Special Publication, 173, pp. 353–384.